RRS Discovery 235c
Cruise Report

RAMESSES II - Reykjanes Axial Melt Experiment: Structural Synthesis of Electromagnetics and Seismics

15th July - 4th August 1998

Christine Peirce

Department of Geological Sciences
University of Durham
Science Laboratories
South Road
Durham
DH1 3LE

christine.peirce@durham.ac.uk

Martin Sinha

Department of Earth Sciences
University of Cambridge
Bullard Laboratories
Madingley Rise
Madingley Road
Cambridge
CB3 0EZ

sinha@esc.cam.ac.uk

January 1999

Table of Contents

List of figures

List of tables

Summary

In late 1993 Peirce (Durham), Sinha (Cambridge) and Constable (Scripps) conducted a combined seismic and controlled source electromagnetic (CSEM) study of a magmatically active Axial Volcanic Ridge (AVR) segment of the Reykjanes Ridge (CD81/93). The target AVR of this study, centred at 57° 45'N, 32° 35'W, was approximately 40 km long and was aligned in an approximately north-south direction. It was chosen originally as being the most magmatically active of the many AVRs that have been identified along the Reykjanes Ridge by seafloor imaging and sampling studies. Analysis of data from this programme revealed the first unequivocal geophysical observations of a crustal magma chamber beneath the axis of a slow spreading ridge. A melt body was clearly evidenced by seismic reflections obtained using a powerful source but a simple receiver (8-channel streamer and 4-fold coverage); by a low velocity zone beneath the axis required by the wide-angle (OBS) data; and by a high-electrical-conductivity zone at a similar depth beneath the axis required by the CSEM data. These results provide a unique opportunity to study the nature of a slow spreading ridge axial melt body beneath a segment that is in the most magmatically active stage of its life cycle - and, in particular, the relationship between the geometry of the melt body, the pattern of seafloor volcanism and the morphological segmentation of the ridge.

During this cruise, D235c, we planned to re-survey the 57° 45'N AVR to obtain a grid of high quality, multichannel seismic reflection profiles along and across the AVR to determine the shape and lateral extent of the axial magma chamber reflector(s) and across adjacent AVRs north and south, including "overlap" regions, to investigate melt continuity. We planned to supplement this dataset with 12 disposable sonobuoy deployments to provide better control of the near surface velocity structure. The integration of these datasets with the 1993 results is expected to lead to major advances in understanding of the process of crustal accretion at slow spreading ridges, and the links between the components of these processes that operate at different depths beneath the surface. Additional geophysical datasets planned consisted of gravity, magnetics and bathymetry. Finally, we planned to undertake a test deployment of two new LEMUR electromagnetic instruments.

During the cruise we acquired 32 across-axis and 5 axis-parallel seismic profiles despite numerous technical difficulties associated primarily with the high pressure air supply. Along each of these profiles bathymetry, gravity and magnetic data were also acquired. Very preliminary observations from the seismic data include numerous intracrustal reflection events similar to those observed during CD81/93, some of which lie solely within the axial region and "overlap" basins between the 57° 45'N AVR and adjacent AVRs north and south, plus Moho reflection events. Both LEMURs were successfully recovered and acquired data according to programming.

1. Introduction and cruise objectives

1.1 Introduction

A large number of sub-sea-bottom geophysical experiments, chiefly seismic, have been carried out on the mid-ocean ridge system over the last decade to investigate the dynamics of crustal accretion, the structure of spreading centres, and the evolution of oceanic crustal structure. Several detailed seismic experiments on fast and intermediate spreading ridges (Harding et al., 1989; Detrick et al., 1987 and 1993; Vera et al., 1990; Kent et al., 1990; Toomey et al., 1990; Burnett et al., 1989; Collier & Sinha, 1990, 1992a,b) have shown dramatically more detail of the structure of the spreading centre than has been achievable before. Features detected include fine structure of the uppermost crust, seismic low velocity zones and reflection events due to a region of partial melt in the middle and lower crust at the ridge axis. Some of these studies (e.g. Kent et al., 1993a,b) have been able to relate structures within the crust to the various scales of morphological and petrological segmentation evident from topographic (e.g. Macdonald et al., 1984) and sampling (e.g. Langmuir et al., 1986) studies. This work has therefore begun to provide some important constraints on the dimensions, physical state and geometry of the crustal melt reservoir and the development of oceanic crustal structure.

In contrast, numerous seismic studies of the slow spreading Mid-Atlantic Ridge (MAR) have, to date, shown little or no evidence for a significant crustal melt body (cf. Calvert, 1995 and Detrick et al., 1990). Indeed Detrick et al. (1990) show that were a melt body reflector comparable to that beneath the EPR present under the MAR at 23°N, it would have been imaged - and was not. Also thermal modelling considerations (e.g. Sleep, 1975; Kusznir & Bott, 1976) have shown that any large, steady-state magma body beneath a slow spreading ridge is unlikely. Clearly MAR accretionary processes as indicated from surveys undertaken thus far, are very different from, and at least as complex as, those on the EPR. Due to the slow spreading rate, the fierce topography associated with the rift valley and large-scale normal faulting, and the probably ephemeral nature of even small bodies of partial melt, progress towards understanding the intracrustal and uppermost mantle processes at slow spreading ridges, including their spatial and temporal variability, is in many ways being made more slowly than for fast and intermediate spreading ridge systems.

The experience of work on other spreading centres has underlined the importance of applying a diversity of methodologies to studies of ridge processes, in order to better understand the complex interactions between magmatic, tectonic and hydrothermal processes that dominate their geology. Our (Peirce and Sinha) work to date on the Reykjanes Ridge, combining seismic techniques (which have the finest spatial resolution of any sub-surface geophysical method) with CSEM (which lacks the resolving power of seismic methods but is uniquely sensitive both to temperature structure and to the presence of interconnected fluid phases - either hydrothermal or magmatic), has revealed for the first time conclusive evidence that geophysically detectable magma bodies do indeed exist beneath slow spreading ridges. The ephemeral nature and long (many thousands or tens of thousands of years) magmatic life cycle of ridge segments has hitherto prevented any studies of the in situ properties of melt bodies beneath the MAR. The objective of this cruise, D235c, was to build upon observations made during the 1993 cruise (CD81/93) in order to determine for the first time the geometry of the axial melt body beneath a slow spreading but magmatically active ridge segment, and its relationship to the shallower level, and more commonly observed, expressions of ridge magmatism - volcanic construction of the seafloor.

1.2 Results from CD81/93

The objective of our original seismic and CSEM study was to investigate the mechanisms of crustal accretion at the axis of the Reykjanes Ridge by determining the physical structure of the crust and uppermost mantle beneath a magmatically active axial volcanic ridge. We selected an AVR centred on 57° 47'N on the basis of swath bathymetry, deep-towed side-scan sonar (TOBI) and gravity data collected by Searle & Parson in 1990. The selected AVR showed clear evidence of widespread, constructional volcanic activity, including hummocky topography, bright back-scattering and fresh-looking lava flows extending for distances of several kilometres. It showed none of the signs of fissuring or faulting that characterise the TOBI data from most AVRs and that appear to indicate post-magmatic, tectonic extension; and it is associated with a negative anomaly in the mantle Bouguer anomaly gravity field. It appeared to be the most magmatically robust of the many well-defined AVRs imaged by the TOBI surveys, and we therefore believed that it represented a segment of the spreading centre that is in the most magmatically active phase of its life cycle. Our choice of AVR was also supported by Murton et al. who dredged freshly extruded lavas from this AVR during cruise CD80/93.

The seismic and CSEM data collected during the CD81/93 cruise (which was funded by the NERC through their normal responsive mode route), have now been processed, interpreted and modelled and reveal unequivocal evidence of a magma body beneath the AVR at 57° 45'N (Sinha et al., 1997,1998; Navin et al., 1998; MacGregor et al., 1998). During CD81/93 coincident wide-angle refraction and reflection seismic data were collected along lines across- and along-axis (see figure 1). The wide-angle data exhibit shadow zones associated with the axis (see figure 2) which can only be modelled by incorporating a low-velocity "melt" body at approximately 2-3 km beneath the axis. The across-axis data indicate that this low-velocity body has a limited extent off-axis – being only ~5 km wide (max. - see figure 3), while the along-axis model reveals that, within the resolution of the wide-angle seismic technique, the data can be modelled by either a distinct low-velocity body or a low-velocity body bounded above and below by a gradient zone. Both of these latter models show that this "melt body" feature extends along the entire AVR (see figure 3). In addition, thinner crust is also required under the axis to satisfactorily model the lower crustal arrivals observed in the OBS data. The normal incidence data collected along both the across- and along-axis wide-angle lines, were shot in an opportunist, piggy-back fashion using only an 8-channel streamer and an airgun array and shot firing interval tuned for wide-angle data collection (i.e. the shot firing rate only enabled 4-fold data coverage to be achieved, while the airgun array was tuned to have the dominant low frequency and high energy suitable for crustal refraction work). Initially, a simple processing scheme was applied to this data to determine the location and thickness/extent of sediment ponds off-axis so that they could be incorporated into the wide-angle initial models. On processing however, using a very crude velocity analysis, distinct reflection events beneath the axis were revealed which were consistent in time with those predicted from the wide-angle modelling. These reflection data have subsequently been processed in greater detail, using velocity information obtained from the coincident wide-angle data and reveal, without any doubt, the presence of sub-axis axial magma chamber reflection events (see figure 4) - the first time they have ever been unequivocally imaged beneath a slow spreading ridge. The combined results of the seismic modelling have been compared with the results of inverting independently the CSEM data. This latter dataset also requires a high conductivity body beneath the axis of the depth and geometry predicted by the seismic analysis, to match the observed data in any way. This combined approach allows us to be confident of our interpretations and their implications. The CD81/93 data thus provide an excellent and unprecedented dataset for studying the physical properties of the crust beneath the AVR along the across-axis wide-angle seismic and CSEM profile. The along-axis seismic reflection profile shows some clear evidence for along-axis variations in crustal magmatic structure, but the existing data are unable to constrain these. The experiment was optimised to provide a 2-D crustal resistivity and seismic velocity section across the centre of the AVR. Extending the results of this study to investigate the along-axis components of the structure of the AVR requires a different approach, with experimental parameters optimised for the new objective.

1.3 Scientific objectives of D235c

The object of this cruise, funded under the NERC's BRIDGE programme, was to return to the Reykjanes Ridge at 57° 45'N and collect a multi-component, multi-disciplinary dataset using the combined resources and expertise of the marine groups at Durham and Cambridge Universities. We aimed to resolve the uncertainties in our current models and also investigate to a greater extent how the existence of a magma chamber relates to the observed surface tectonic and accretionary processes. The scientific objectives are many fold, but can be summarised as follows:

(i) Is the "melt" body continuous along the AVR as predicted by the wide-angle data or segmented as imaged in the poor quality seismic reflection data?
(ii) What happens to the axial melt body close to offsets at each end of the AVR (cf. Collier and Sinha, 1990, 1992a,b)?
(iii) What are the physical properties and state of the material within, above and below the melt body?
(iv) How does the porosity of the upper crust – which is likely to be the source region for a hydrothermal circulation system – vary with depth and across the AVR?
(v) Are any intracrustal seismic reflectors present that can be related either to magmatic or tectonic activity?
(vi) What is the nature of the Moho transition along an across-axis traverse and what does it reveal about Moho development as a function of age? Does the Moho shallow towards AVR tips and is it shallower beneath the axis than off-axis? If the crust is thinner beneath the axis, as indicated by the across-axis wide-angle refraction data modelling, does this imply that melt gets into the crust to continue thickening it out to distances of tens of kilometres from the axis? If this is the case, might we

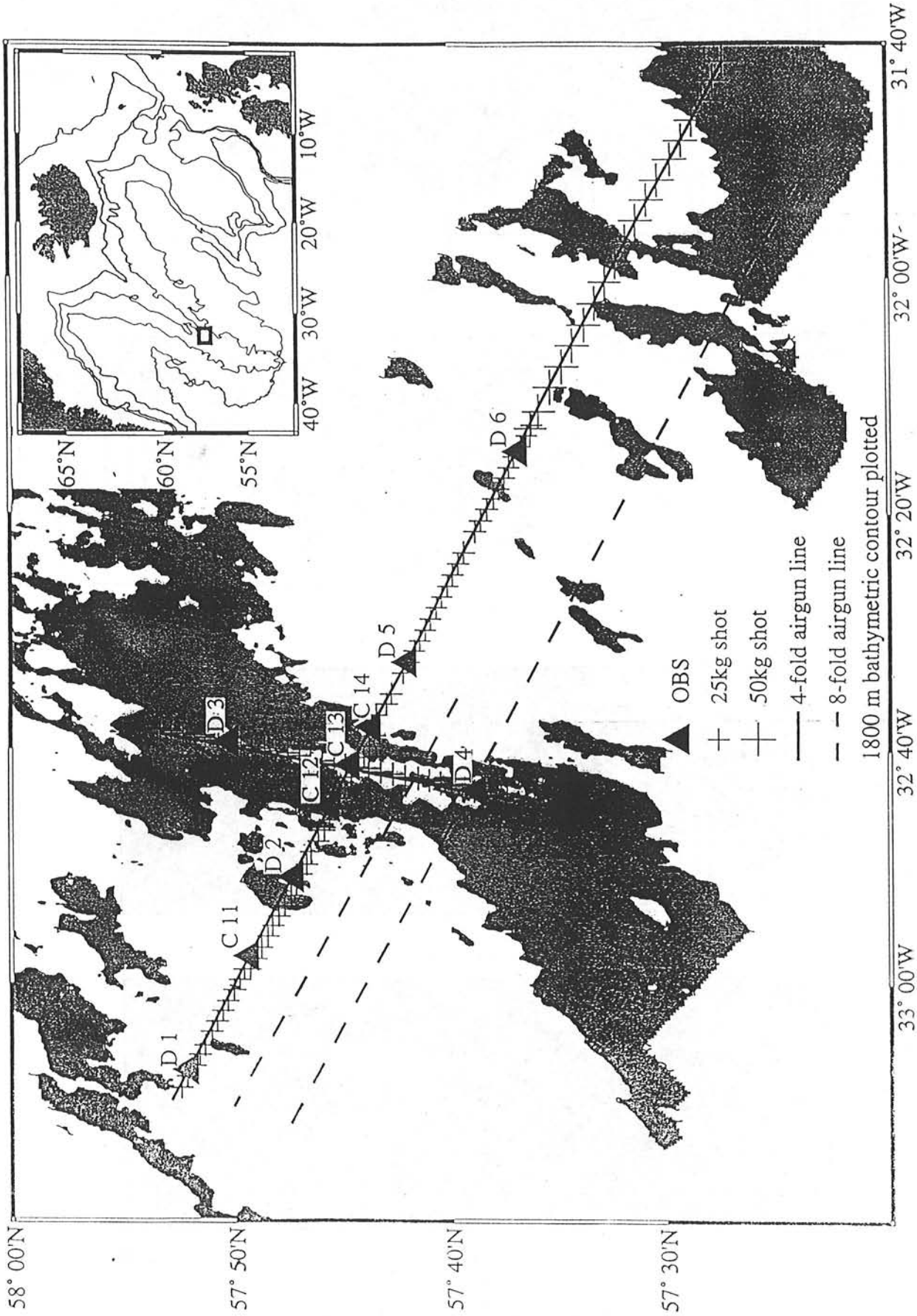

Figure 1. CD81/93 seismic profiles.

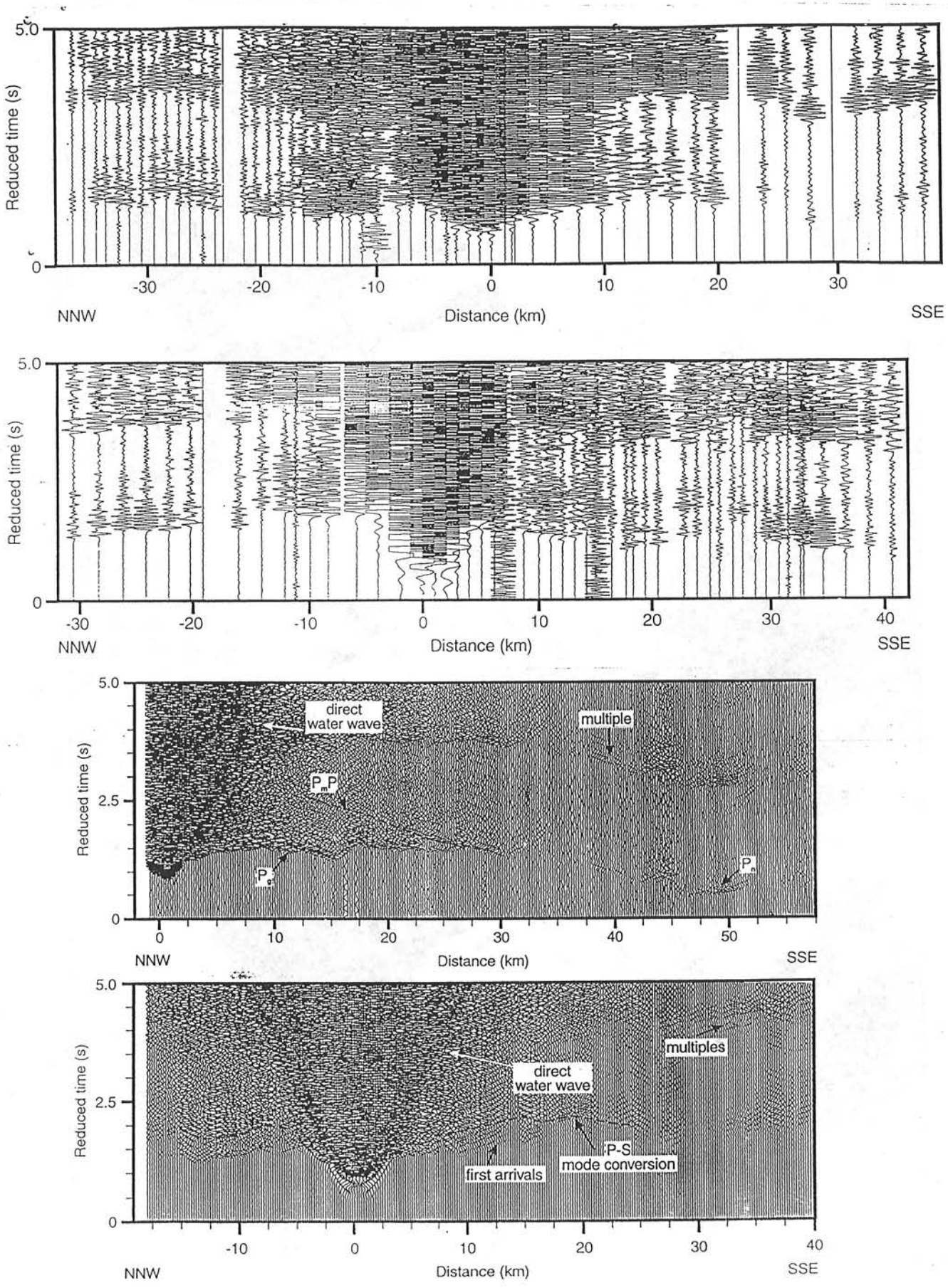

Figure 2. Example CD81/93 wide-angle seismic data.
UPPER: explosive data.
LOWER: airgun data.

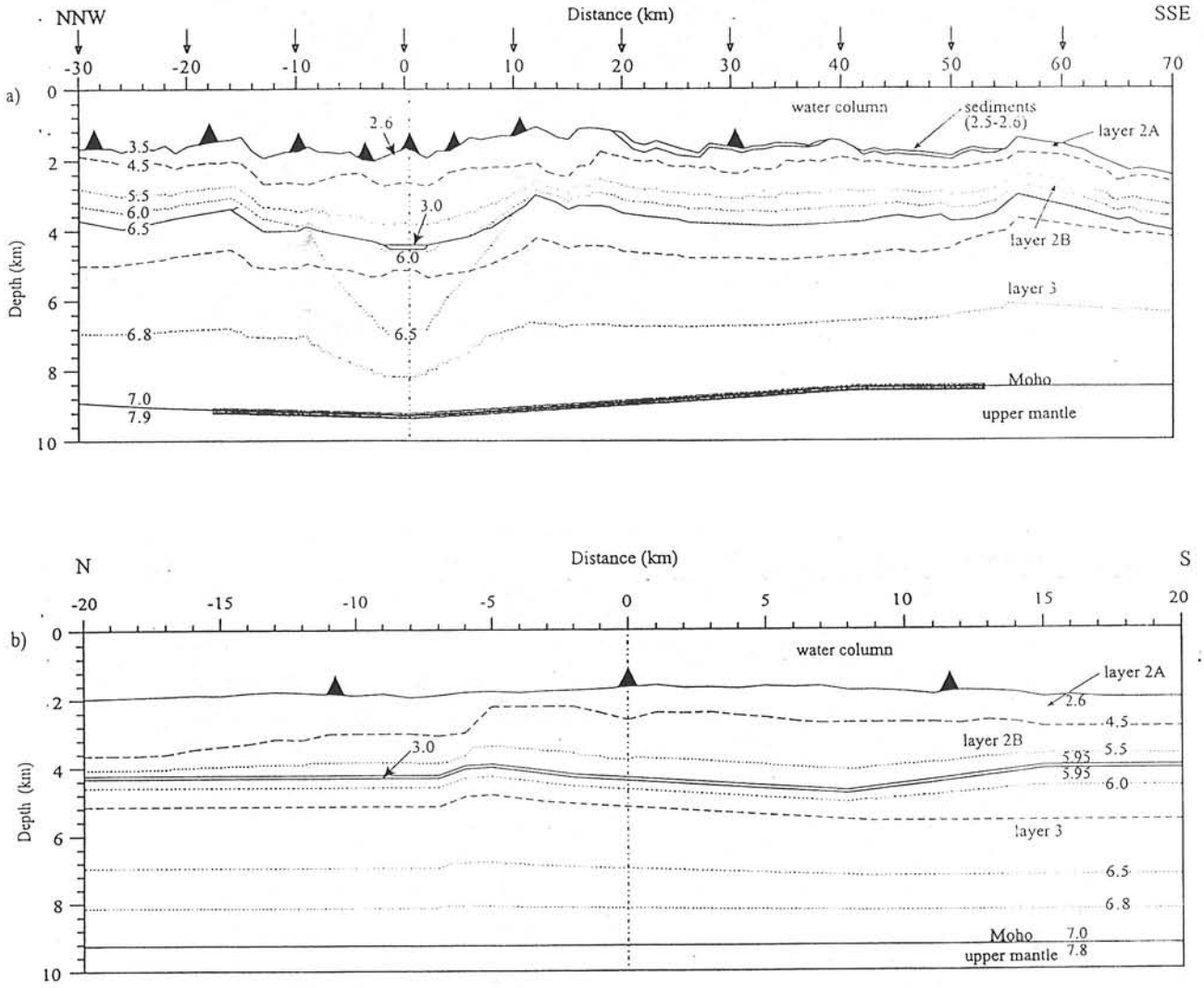

Figure 3. CD81/93 best-fit velocity-depth models. Isovelocity contours are in kms^{-1}.
UPPER: across-axis.
LOWER: along-axis.

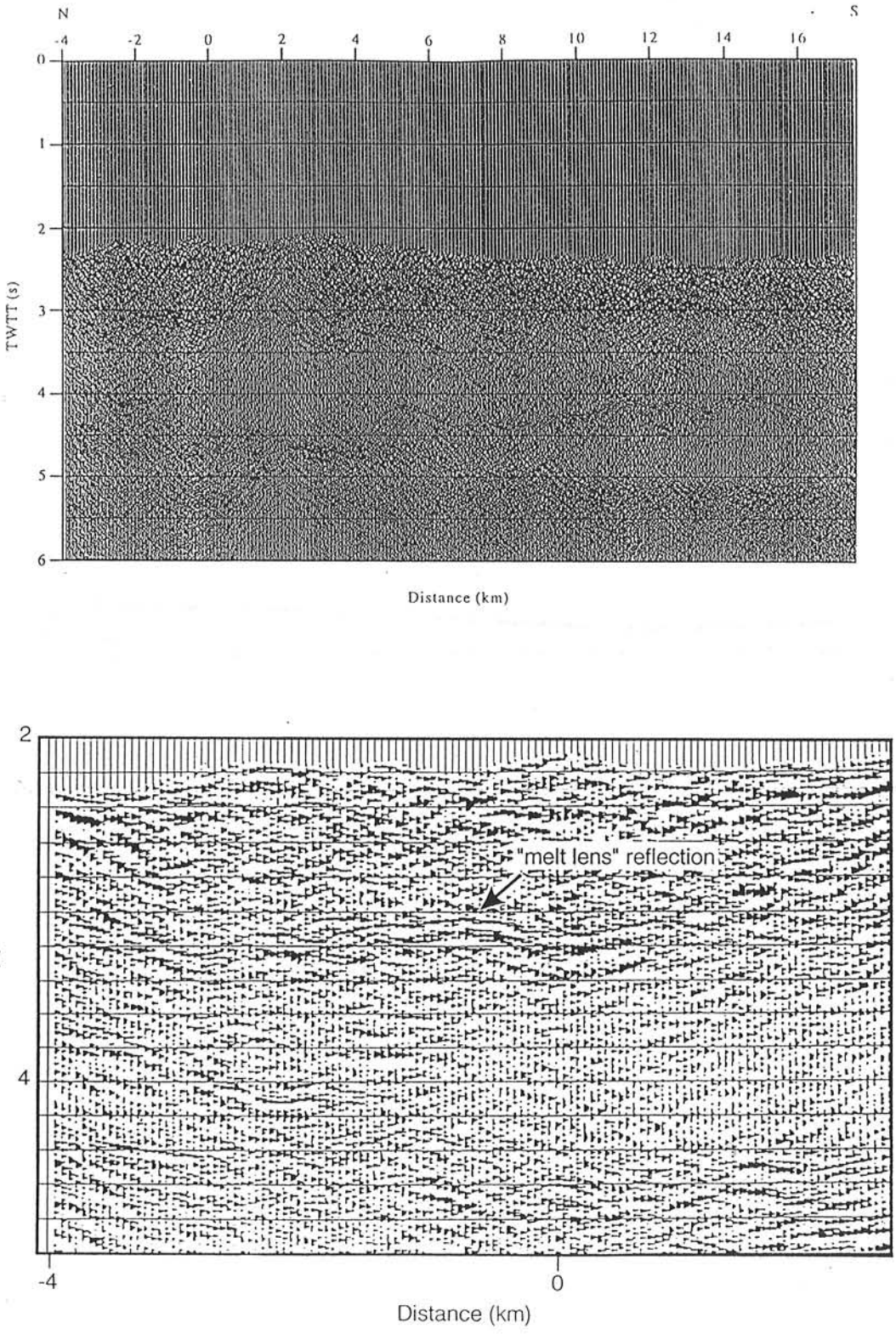

Figure 4. CD81/93 seismic reflection data.
UPPER: part of the four-fold along-axis line showing the melt lens reflection event.
LOWER: enlargement of the melt lens reflection event shown above.

expect to see either intracrustal melt bodies, or melt ponding at the Moho off-axis (cf. Garmany, 1989)? Evidence of normal faulting in layer 2 a few kilometres off-axis has to date, lead us to expect the crust to be stretched and thinned as it moves off-axis; this is the exact opposite of what our seismic models imply, i.e. that the crustal accretion zone at 57° 45'N on the Reykjanes Ridge is tens of kilometres wide, with most of the melt being injected at the axis but with significant amounts still intruding/underplating the crust out to ages of 2-3 Ma (cf. at the EPR at 9° 30'N, where both normal incidence and wide-angle data have imaged the Moho, the crust appears to reach its "normal" thickness within two to three kilometres off-axis, i.e. within a few hundred thousand years, and where any observed crustal thickening can be related to layer 2A).

(vii) How are the sub-surface accretionary processes related to surface features? Do the melt bodies correlate with a characteristic set of surface features which will allow melt body location at other slow spreading centres by means of seabed images alone?

(viii) Can detailed high-resolution crustal magnetisation observations around the AVR be used to further characterise the axial magma chamber(s) (cf. Tivey and Johnson, 1987)?

(ix) Can detailed mapping of the Brunhes/Matuyama and Matuyama/Gauss magnetic reversal "transition widths" be used to investigate volcanic emplacement processes and date lava flows (cf. Macdonald et al., 1983; Searle et al., 1994)?

(x) Why do AVR associated faults change from AVR-parallel to axis-parallel geometries with age (cf. Searle and Laughton, 1981; Murton and Parson, 1993)?

and finally

(xi) What can we learn from all of these about the processes of melt formation, migration, accumulation and emplacement, and the construction and evolution of oceanic crust at the Reykjanes Ridge and slow spreading ridges in general?

We planned to address objectives (i) - (v) by detailed processing and interpretation of multichannel seismic reflection data collected along numerous 2D lines across and along the entire AVR at 57° 45'N and in the overlapping regions between adjacent AVRs (figure 5). We will use this data primarily to develop 3D maps of magma chamber location and consistency along- and across-axis in an attempt to resolve the contradictions between the current wide-angle and normal incidence data interpretations. We will also conduct sub-gather amplitude versus offset modelling to determine the nature of the material within, above and below the "melt" body to determine not only the physical state of the material but also whether it is contained within a distinct chamber or a gradual transition zone - neither of which is currently resolvable from the 4-fold, extremely limited offset gathers or the wide-angle data.

The nature of the Moho transition [(vi)] and how it develops with oceanic crustal age will also be addressed using the multichannel reflection data. The existing wide-angle models imply that a distinct Moho exists directly beneath the ridge-axis, i.e. at zero-age. The Moho in each of the models is well constrained along their entire length by many crossing ray paths which allows us to have confidence that this in fact the case. However, the nature of the P_mP and P_n phases observed do not allow us to map this boundary as a function of depth and offset with any degree of accuracy (i.e. ± 1 km depth at best) and hence, the nature of the dip on this interface and the exact crustal thickness along-axis is uncertain. The wide-angle models predict that the Moho reflection will arrive between about 4-5 seconds TWTT, just above the sea-surface/seabed multiple, which may be one reason why it isn't obviously resolvable on the existing 4-fold data, that combined with the restricted sub-gather offsets. However, although the Moho reflection will be close in time to the multiple, the variations in water depth along all our lines should ensure that we are able to observe it in most places, although it may be obscured in others.

Finally, it is important to address how the sub-surface processes relate to the observed seabed features (i.e. lava flows, the density variations of well-constructed volcanoes along the AVR and off-axis etc.) and how they can allow us to map foci of accretionary activity [(vii)-(xi)]. The AVR at 57° 45'N appears from previous TOBI work to be a pristine AVR, offering the opportunity of completely characterising the young end-member in the AVR evolutionary sequence. However, the EW9008 TOBI survey covered only the northern half of this AVR. Good side-scan data were obtained, but there is only poor single component magnetic data coverage. We planned to complete the magnetic coverage of this AVR (including the northern part) by collecting data along every seismic line shot. Swath bathymetry and side-scan sonar data gridded from CD81/93 and EW9008 will thus be used to determine the detailed volcanic morphology, including the ratio of small hummocky ridges (fissure volcanoes) to larger conical and flat-topped volcanoes which, according to Parson et al. (1993), should be low for a young AVR. Covering the whole AVR will allow us to investigate along-axis variations in

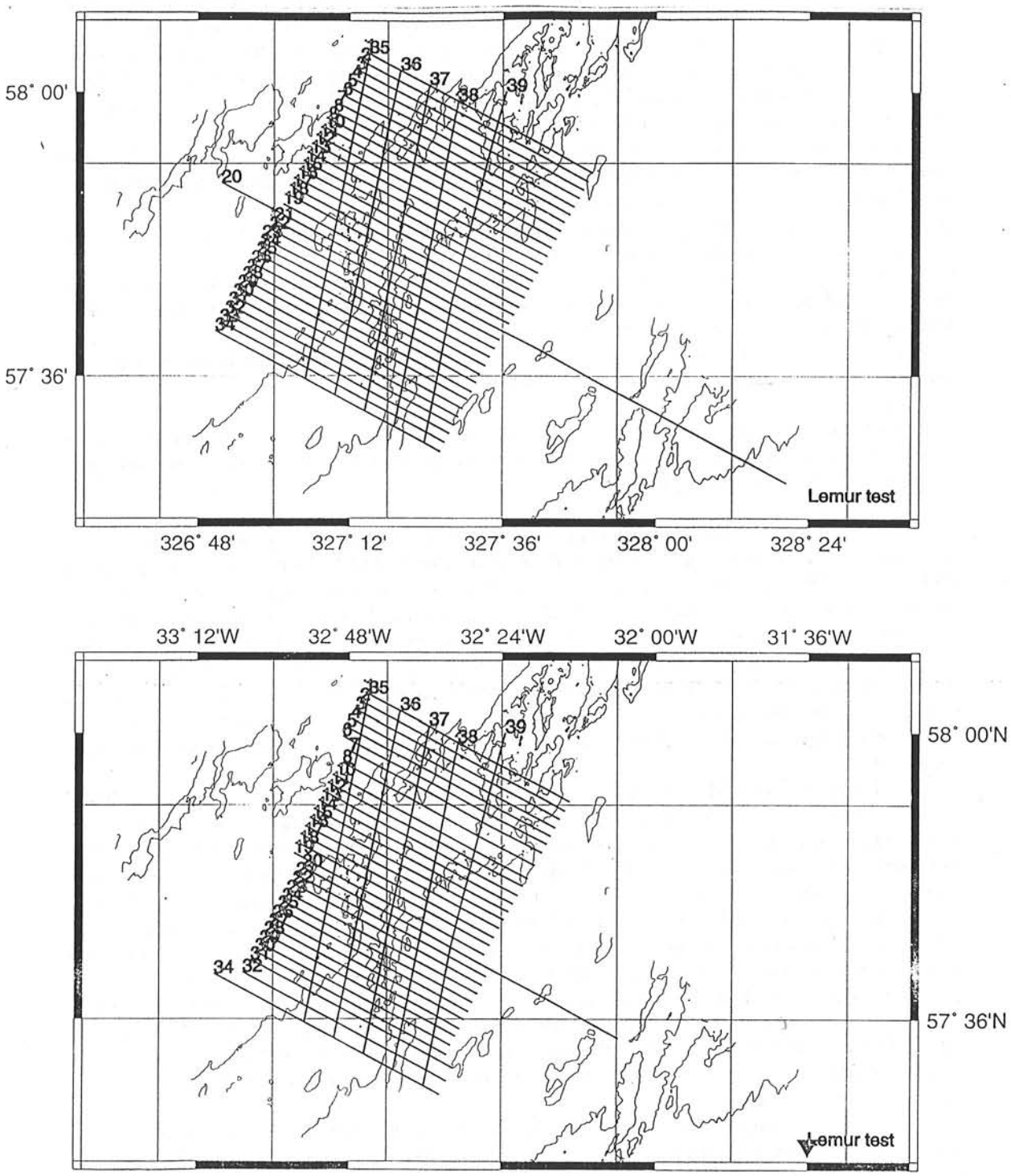

Figure 5. Pre-cruise seismic line locations a) pre-shortening and b) post-shortening, due to the progressive loss of shooting time resulting from last minute port call and departure and arrival time changes.

morphology and thus test hypotheses of ridge accretion (e.g. the "Icelandic fissure swarm" model of longitudinal dyking away from central volcanoes predicts a predominance of central volcanoes near the AVR centre and fissure volcanoes near its ends). The swath bathymetry data in conjunction with the seismic, gravity and magnetic data will enable a more quantitative analysis of morphology than before. We will also use the magnetic data to investigate AVR architecture and spreading rate vs. time. By comparing variations in apparent AVR age and degree of faulting along-axis, Parson et al. (1993) derived a model of AVR development. By extending our coverage off-axis we will test this model, examining several clearly-defined relict AVRs that can be seen off-axis in the swath bathymetry data already collected in this area. We will especially investigate the detailed nature and development of off-axis faulting and the change from AVR-parallel to axis-parallel faulting (Searle and Laughton, 1981), extending to greater ages than were available to Murton and Parson (1993), whose results we will test. We will also investigate details of the Brunhes/Matuyama and Matuyama/Gauss magnetic reversal "transition widths" and hence infer the effective width of the volcanic emplacement process (Macdonald et al., 1983; Searle et al., 1994).

1.4 Methodology

We planned to address the scientific objectives of this cruise by combined use of multichannel seismic reflection, magnetic and gravity methods over the AVR centred at 57° 45'N on the Reykjanes Ridge. The experiment consisted primarily of the use of RVS' 2.4 km long streamer and associated multichannel reflection profiling system.

In the first instance we planned to collect a grid of across-axis lines spaced at approximately 1.5 km intervals along the entire length of the AVR at 57° 45'N (see figure 5). One of these lines we planned to extend off-axis and locate it along the existing coincident wide-angle refraction and 4-fold reflection seismic profiles. The re-shoot line was designed primarily to better constrain the melt body reflector already imaged and the crustal structure models obtained using existing data (see figures 3 and 4), while also imaging the variation in crustal structure and Moho depth as a function of age (i.e. 2-3 Ma off-axis). Re-shooting this line (line 20) should also provide a velocity-depth reference for the remaining 33 across-axis lines. The across-axis lines form a grid enabling the continuity in the crustal magma body to be investigated along the entire length of the AVR. A number of these lines were located north and south of the termination of the AVR to investigate magma chamber continuity between adjacent AVRs. We planned to tie the grid together by a number of approximately north-south lines running AVR-parallel. All lines were planned to run along the entire AVR length and the central line would re-shoot the other existing coincident wide-angle refraction and 4-fold reflection lines collected during CD81/93 (see figure 1). The remaining lines would be shot at 5 and 10 km off-axis to investigate the structure of the crust within and outside the median valley. Using the collected multichannel data we should be able to construct a detailed 3D model of the AVR up to 20 km off-axis.

We planned to configure the streamer for seismic reflection data collection so that we could also use individual shot gathers to conduct a detailed amplitude versus offset (AVO) analysis, especially of the along-axis line, to investigate the physical state and properties of the material in and above the melt body using forward modelling techniques. Amplitude versus offset characteristics of a melt body reflection event will contain much useful information about the physical state of the melt body, based on the respective reflection coefficients and their angular variations at the top and (if present) bottom boundaries of the melt body. To achieve maximum sub-gather offset traces with the RVS streamer we planned to supplement the dataset with data recorded by deployed sonobuoys. We also planned to optimise the firing rate to maximise the data fold. The original shot firing plan was scheduled to take 15 days. The shooting order of the lines would also be optimised to minimise the length of time spent turning.

1.4.1 Pre-cruise changes to the scientific plan

A number of factors prior to the cruise combined to shorten the shot firing period considerably from that sought in the original application. Due to the initial air volume requirements and restrictions imposed by the existing ship time programme, the cruise was scheduled in July-August on the *RRS Discovery*, with port calls in Fairlie (pre-cruise) and Southampton (post-cruise). As limited funds were available from the BRIDGE programme for this cruise and ship time on the *Discovery* costs significantly more than the *Darwin*, the cruise was immediately shortened to the bare minimum considered viable to undertake the originally proposed work and for which there were sufficient funds remaining - 10 days in the work area. However, without consultation with either of the PIs, the pre-cruise port call was moved to Southampton by RVS for financial reasons related to mobilisation. This added an extra day to the passage and effectively removed half of the contingency time that we had

built into the surveying schedule. These factors combined to result in the across-axis lines having to be shortened by up to 6 km (3 km on each end) to enable the planned lines to be shot in the remaining time frame (figure 5). In addition, we discovered at fairly short notice prior to the cruise that we would not sail until the afternoon of the "departure" day and that we must arrive by 8 am on the "arrival" day. This had the effect of removing all of the remaining contingency time. Finally, despite funding being available from the University of Durham for an additional day of surveying, this could not be accommodated within the programme due to restrictions imposed by the ship's attendance at EXPO'98 immediately after D235c.

The line shooting order (Table 3) had thus to be revised to optimise the time now available for shooting - ~8 days - i.e. minimise the time spent making turns and passaging between adjacent lines or between across-axis and along-axis lines. In an attempt to add some contingency into the shooting schedule we decided to shoot every third line across-axis for two reasons: a) it resulted in a 4.5 km line spacing between "adjacent" lines such that a turn rate of 4°/min would always be achieved; and b) the grid of across-axis lines would be shot in three passes thus, if major equipment problems or bad weather were experienced, we would be able to survey the entire AVR and adjacent areas, even if at a greater line-to-line spacing - a contingency plan created from no remaining contingency time.

1.4.2 Intra-cruise changes to the scientific plan

By comparing the chart of lines shot during D235c (figure 7) with that planned prior to the cruise (figure 5), some notable differences can be observed (compare also Table 3 and Table 4). The main deviations are related to the onset of major equipment failure and its progressive deterioration after repeated repair. The majority of the failure is attributable ultimately to the air supply and the compressors themselves, and this will be discussed further in Section 4. As far as the cruise plan is concerned this equipment failure resulted in a number of lines not being shot at all, a number of lines being shot at a longer shot interval, a number of lines being shot in several overlapping parts, and a redesign of the shot firing plan while surveying to optimise the time remaining (on advice from the onboard technical staff) such that our most desired lines were shot before the situation became irretrievable. See Section 2 below.

1.5 Mobilisation

Mobilisation for the cruise revolved mainly around loading and installation of the airgun array and multichannel streamer. In addition, prior to the pre-cruise mobilisation period *Discovery*'s compressors also required reassembly, testing under load and recertification of the air bottles as they had been mothballed due to lack of use over the previous three years. This mothballing took place despite recommendations made in previous cruise reports that the compressors should be routinely maintained and run by the ship's engineers as part of the ship's onboard machinery/equipment.

As a result of staff availability, the majority of the major equipment commissioning was left until just prior to the cruise, including the final stages of commissioning the compressors (the air bottles were not certified until the day before we sailed). In fact departure was delayed in an attempt to "iron out" problems related to the compressors' computerised management system, which only allowed the compressors to be run up at the running speed. Under normal ship's engine running levels this had the effect of blacking out the whole ship, an event which occurred twice while still in port. Thus to start the four onboard compressors, all of the ship's engines had to be running.

On arrival pre-cruise in Southampton it became clear to the PIs that there had been, and still were, major problems associated with mobilising for this cruise, some of which were related to preparation for the ship's visit to EXPO'98 immediately after the cruise. Staff morale was exceedingly low with, in addition, technical staff being brought in from outside to prepare and undertake equipment deployment at sea. Expressions of surprise were also made to both PIs that preparation had got as far as it had. It became clear that this cruise was only taking place due to the dedication, goodwill and pride-in-the-job attitude of the remaining technical staff at RVS, both sea-going on this cruise and not, who appear to have been placed in an untenable position, particularly those sailing on this cruise and forced to make "the best of it". There was a five day passage to and from the work area which eased the port call mobilisation/demobilisation somewhat.

2. Work conducted and data collected

2.1 Multichannel seismic experiment

Prior to the cruise a shot firing interval of 15 s was selected to provide 32-fold data using RVS' 96-channel streamer which has a 25 m group interval. In addition, the configuration and construction of the airgun array was forward modelled for source signature and energy, to produce the optimum possible with RVS' selection of chamber sizes and towing parameters for the melt lens target size and depth below seabed. Figure 6 shows the airgun array configuration. In addition, the optimum towing depth of the streamer in relation to the array was also modelled (see figure 6). None of these towing parameters were achieved for a variety of reasons and these will be discussed further in Section 4.

Figure 7 shows the grid of lines actually collected during D235c. Any deviations from the planned lines or shooting order were solely due to equipment failure, the causes of which will also be discussed in Section 4.

On first inspection the "quick look" processed (figure 8) data show a number of interesting features and the dataset appears to be of high quality. Even with basic processing, intracrustal reflection events associated with the melt lens depth as modelled from the CD81/93 dataset can be clearly observed on the majority of the across-axis and on the along-axis profiles. In addition, an intracrustal reflection event can be imaged beneath the 'overlap' regions between adjacent AVRs. Also, Moho reflection events are also observed to the west of the survey area.

2.2 Sonobuoy deployments

Throughout multichannel surveying twelve sonobuoy deployments were planned not only to provide detailed velocity information on upper crustal structure but also, along the along-axis line (line 37), to provide large shot-receiver trace offsets for amplitude vs. offset analysis for melt lens/magma chamber properties. Unfortunately the hand deployment strategy solely available on NERC' ships resulted in all of the deployed sonobuoys not surviving for more than about 10 min., due largely to collision/entanglement with component parts of the multichannel acquisition system. Despite numerous and varied attempts to increase the lateral deployment distance (e.g. by using the ship's crane or by deploying from the "outside" side of the ship whilst turning) no sonobuoy deployments were successful.

2.3 LEMUR test

As part of another project (the ISO-3D project which is jointly funded by NERC and the European Union's MAST-3 programme), Sinha and others at Cambridge are currently making some improvements to the Cambridge LEMUR (Low-frequency ElectroMagnetic Underwater Receiver) instruments. These instruments are used as receivers during controlled-source electromagnetic sounding studies of oceanic crust. LEMURs are autonomous ocean-bottom instruments, which record the AC electric fields at the sea floor generated by a deep-towed source system. Each LEMUR has two, 13 m, orthogonal horizontal electric dipole receiving antennas; four Ag/AgCl low noise, non-polarising electrodes; and a logger system with 24-bit analogue-to-digital conversion and mass storage of data on hard disk drives. The instruments free fall to the sea floor, and are recovered at the end of an experiment by acoustic release units which can be commanded from the ship to release the instrument's bottom weight, allowing the main instrument package to float back to the surface for recovery.

During cruise D235c, we took the opportunity of carrying out sea trials of the modified LEMUR instrument, prior to constructing six new instruments for a cruise in 1999. One of the major changes to the instruments is their mechanical layout, which has been substantially modified to improve ease of handling at sea. The prototype of the new system was built in the first half of 1998, and sea tested on this cruise by means of a single deployment. The new instrument frame was fitted with two discrete LEMUR recording instruments, and deployed in approximately 2700 m of water on the eastern flank of the Reykjanes Ridge for 14 days. Although in normal use the system will have only a single recording package, the advantage of deploying two instruments on one frame is that it is then possible to assess the coherence between two independent recordings of the electric field. This makes it possible to distinguish between noise that is generated internally within the instrument (which is not coherent), and ambient or environmental noise at the sea floor (which should be coherent).

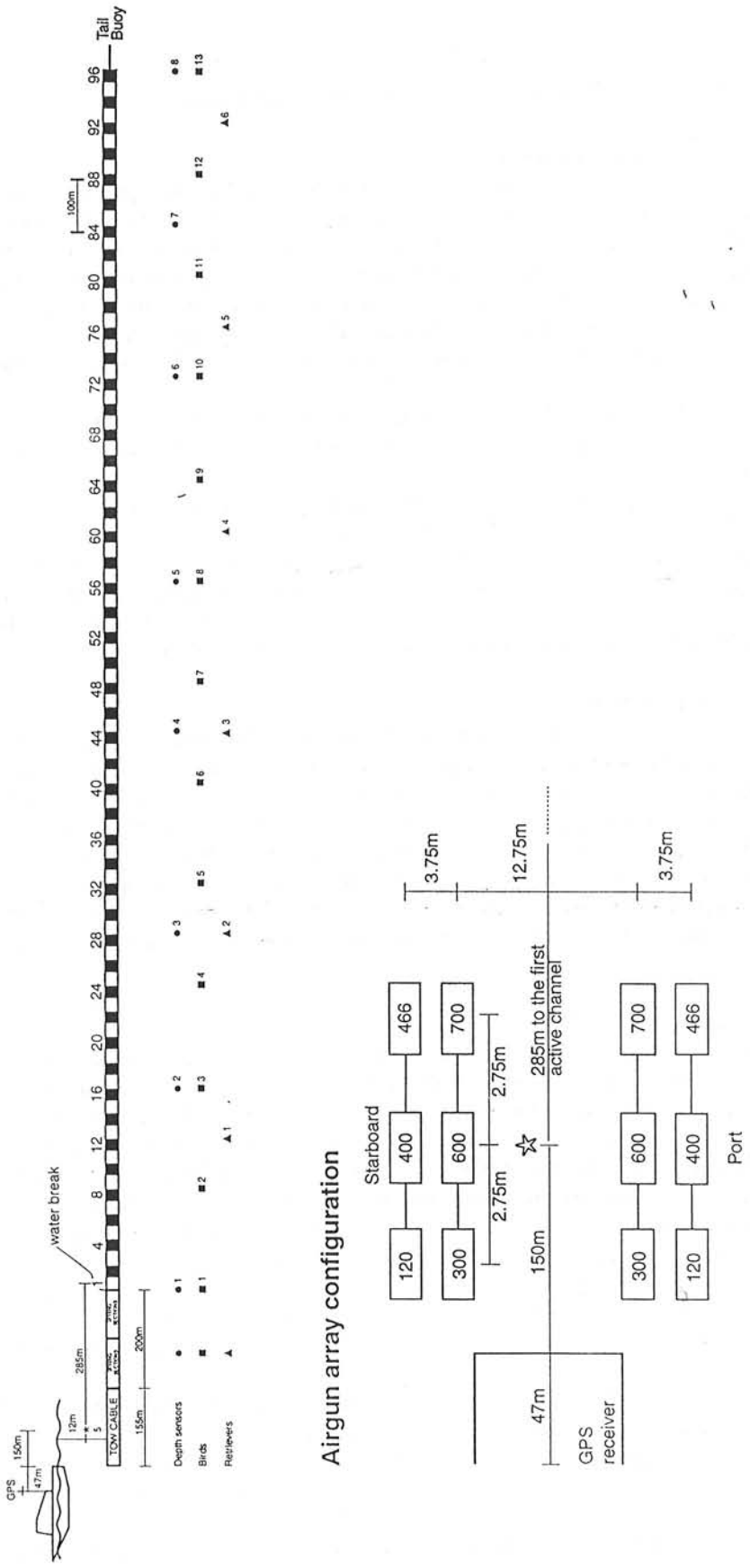

Figure 6. Airgun array and multichannel streamer configuration modelled and requested for D235c.

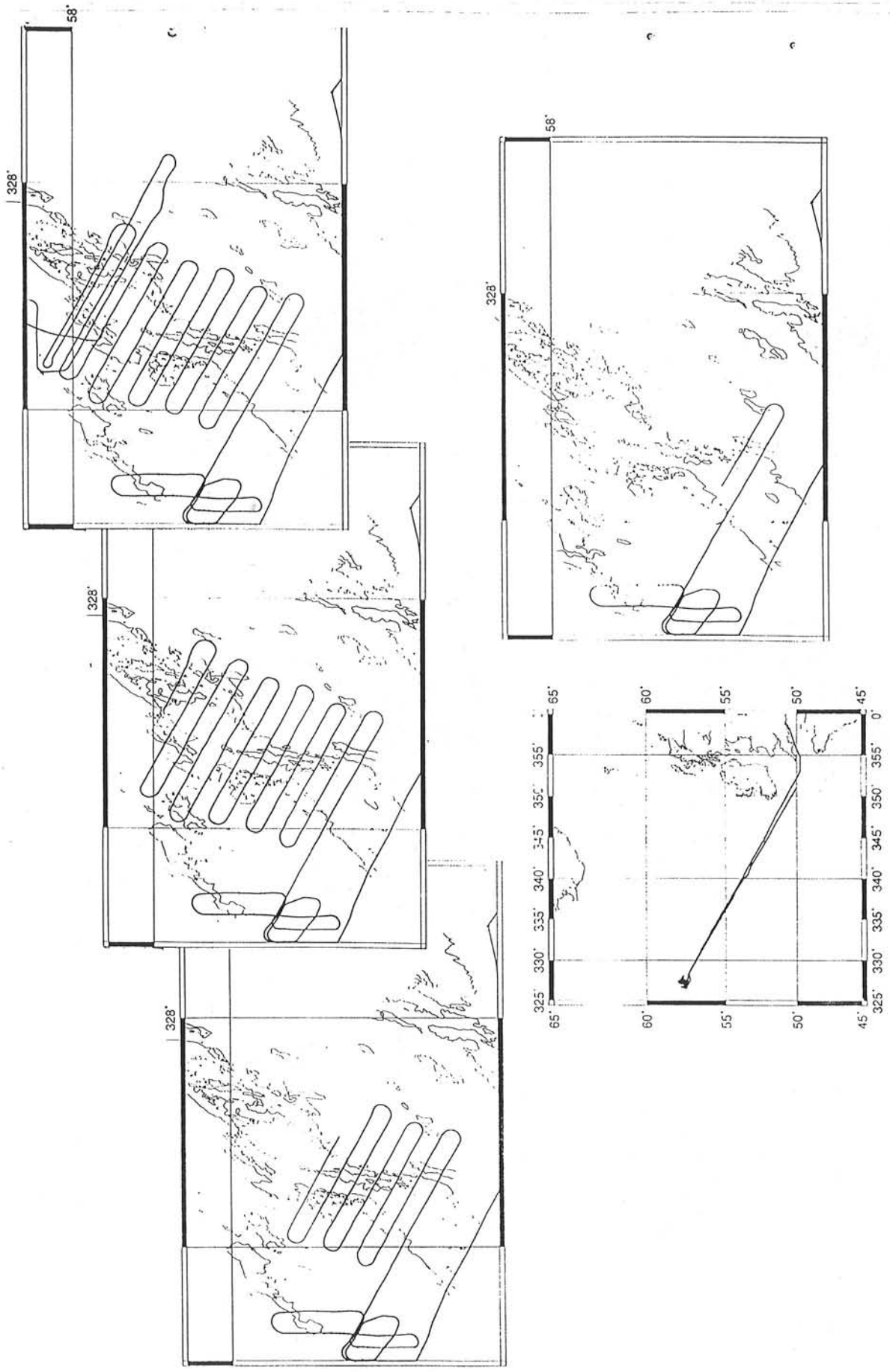

Figure 7. Seismic lines shot during D235c. The individual plots show how data coverage was achieved by three across-axis passes and one along-axis pass to optimise ship time and maximum turning rate.

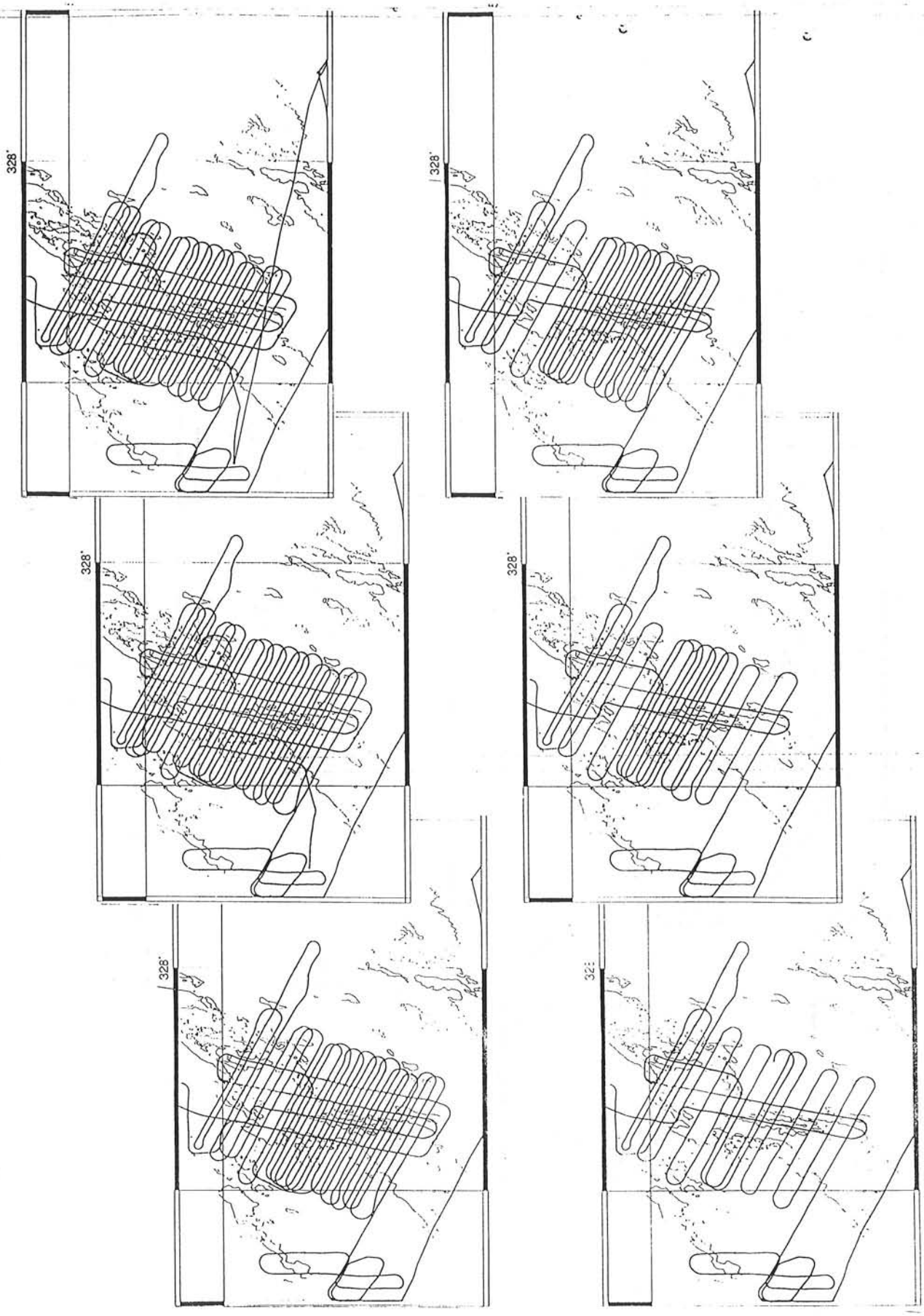

Figure 7 cont.. Seismic lines shot during D235c. The individual plots show how data coverage was achieved by three across-axis passes and one along-axis pass to optimise ship time and maximum turning rate.

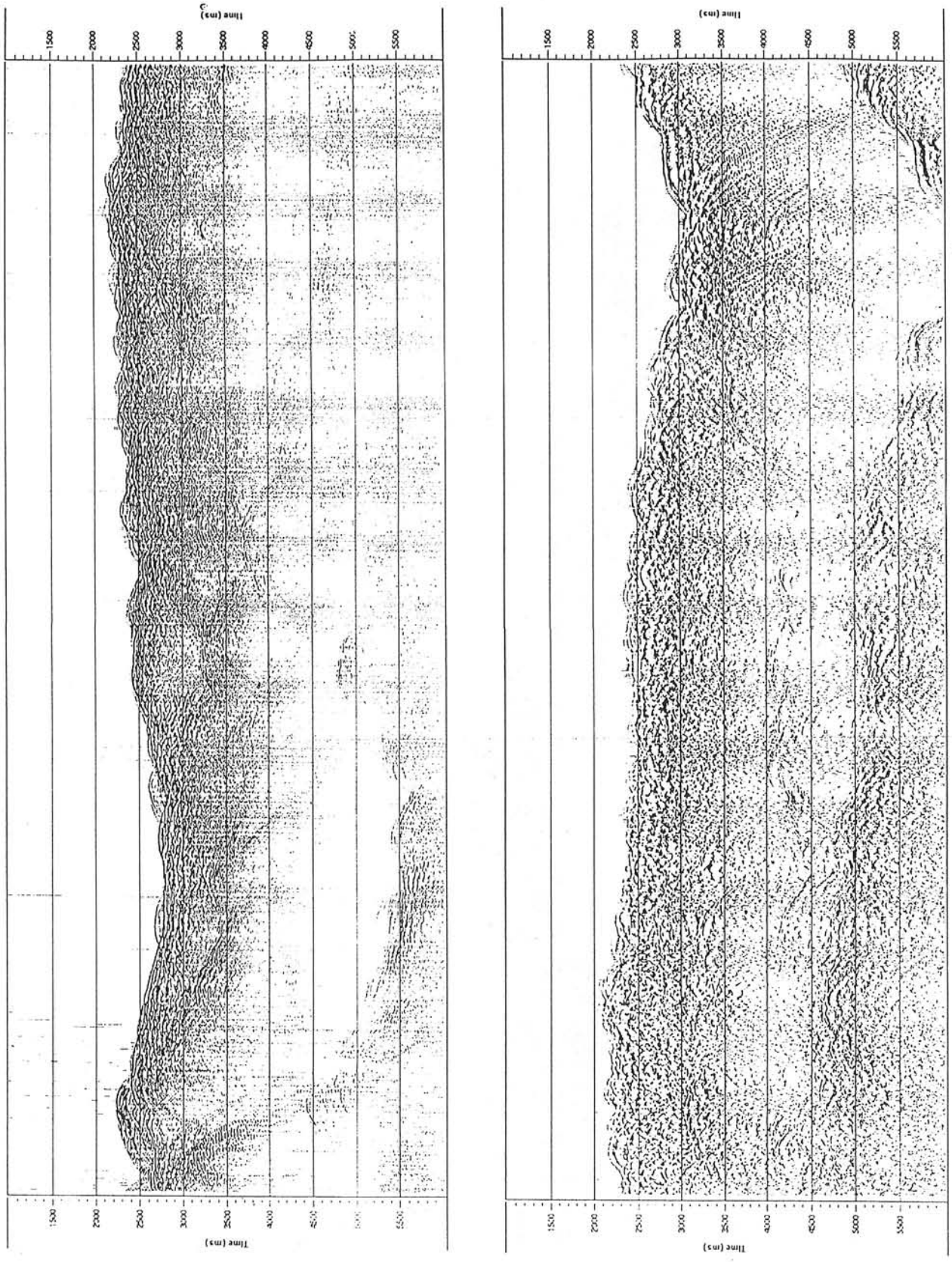

Figure 8a. UPPER: along-axis (line 37 - see figure 5) near-offset single channel trace monitor from D235c, plotted north-south. LOWER: Four-fold stack of the along-axis data for CD81/93, plotted south-north.

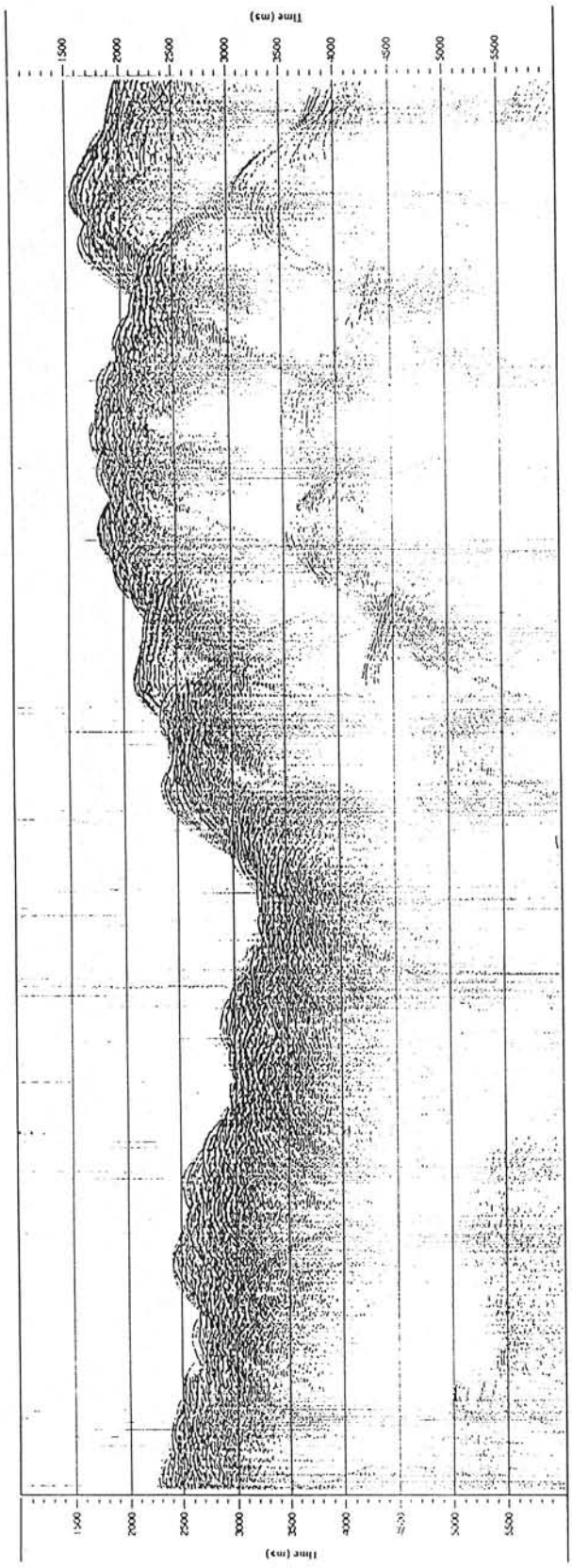

Figure 8b. Single channel near-offset trace monitor of line 31 (see figure 5), shot east-west.

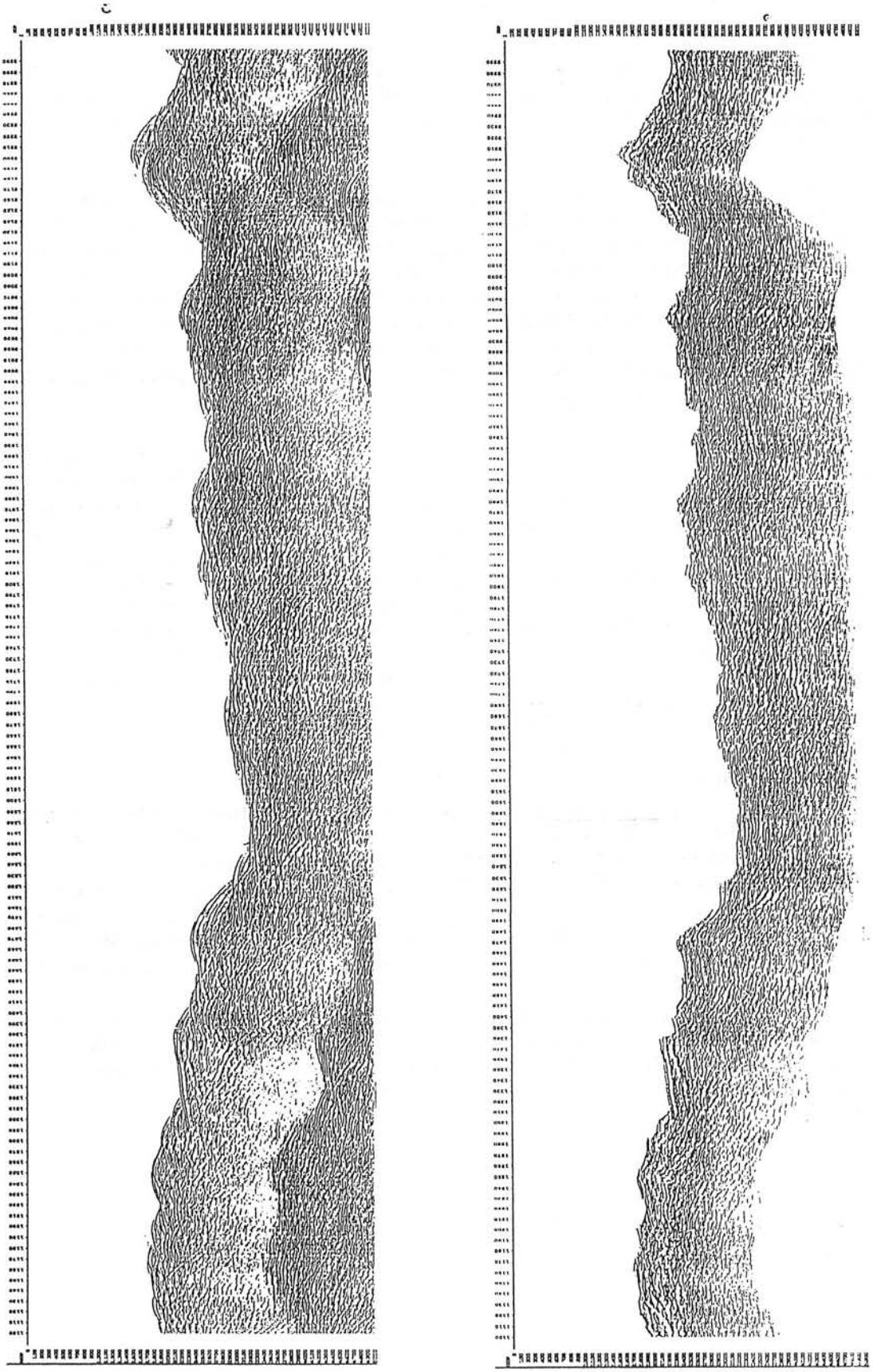

Figure 8c. Processed data from line 34 (see figure 5).
UPPER: 1500 ms^{-1} brute stack. LOWER: 1500 ms^{-1} brute migration.

The test was fully successful. Both recording systems worked for the duration of their programmed periods, completely filling their disks with data. Handling of the new frame and bottom weight assembly was straightforward, confirming that the new design will greatly ease operations at sea. The instrument was recovered without difficulty. Figure 9 shows two photographs of the test deployment.

Figure 10 is a noise spectrum, showing the amplitude in Vm^{-1} as a function of frequency, across the range of frequencies to be used in the 1999 controlled source experiment. LEMUR 11 and LEMUR 15 were the two discrete instruments deployed in tandem for the test. Channels 1 and 2 represent the two orthogonal components of horizontal electric field, measured by a total of 8 electrodes across two 13 m dipoles. The response of both channels and both instruments is similar, as expected. At frequencies above 3 Hz, the noise level is $<10^{-10}$ Vm^{-1}, and the spectrum is generally red, also as expected due to the screening of externally generated fields by the water column. There is a pronounced peak in the spectrum at 0.75 to 1 Hz. This component of the signal appears and disappears through the records, with durations of a few hours. We suspect that this is noise induced by water currents passing over the instrument.

Figure 11 is a plot of the coherence between the two independent recordings of each dipole. It shows correlation coefficient (calculated from amplitudes only) as a function of frequency across the same frequency range as the last figure. It can be seen that, at 0.75 Hz to 1 Hz, the noise is coherent between the two recordings, and at higher frequencies the coherence falls off sharply. Our conclusion is that the noise peak at 0.75 Hz to 1 Hz is due to motionally induced fields. At higher frequencies, noise levels are generally lower, the time series are not coherent, and the observed noise values are probably dominated by internally generated instrument noise rather than environmental noise.

The noise levels of $<10^{-10}$ Vm^{-1} at frequencies of 3 Hz and above, combined with the DASI source moment of $>10^{4}$ Am, confirms that - given similar conditions during our 1999 experiment - it should be possible to record data at signal levels down to less than 10^{-14} V $A^{-1}m^{-2}$ - comparable to the best results achieved from any previous oceanic CSEM experiment.

Table 2 summarises the deployment parameters for this instrument test.

2.4 Additional datasets

The primary objective of the cruise was to carry out the multichannel seismic experiment outlined above. However, throughout the cruise we also collected both gravity and magnetic datasets. Gravity data were collected throughout the cruise from pre-cruise port call to just before arrival back in Southampton. Total field magnetic data were collected throughout seismic data acquisition only. In addition, bathymetry measurements were made along each seismic profile and these will be merged with the existing CD81/93 and EW9008 swath bathymetry datasets, to provide a detailed 3D image of seabed topography vital to multichannel seismic data processing and interpretation in mid-ocean ridge environments.

Finally, 24 XBT (Expendable Bathymetric Thermographs) measurements were also made at the locations shown in Table 5, to provide a detailed image of the water column structure throughout the work area. Unfortunately, a number of these XBT deployments failed due to entanglement with both the multichannel streamer and, more particularly, the airgun array.

Figure 9. Photographs of the modified LEMUR instrument, during its deployment during D235c.

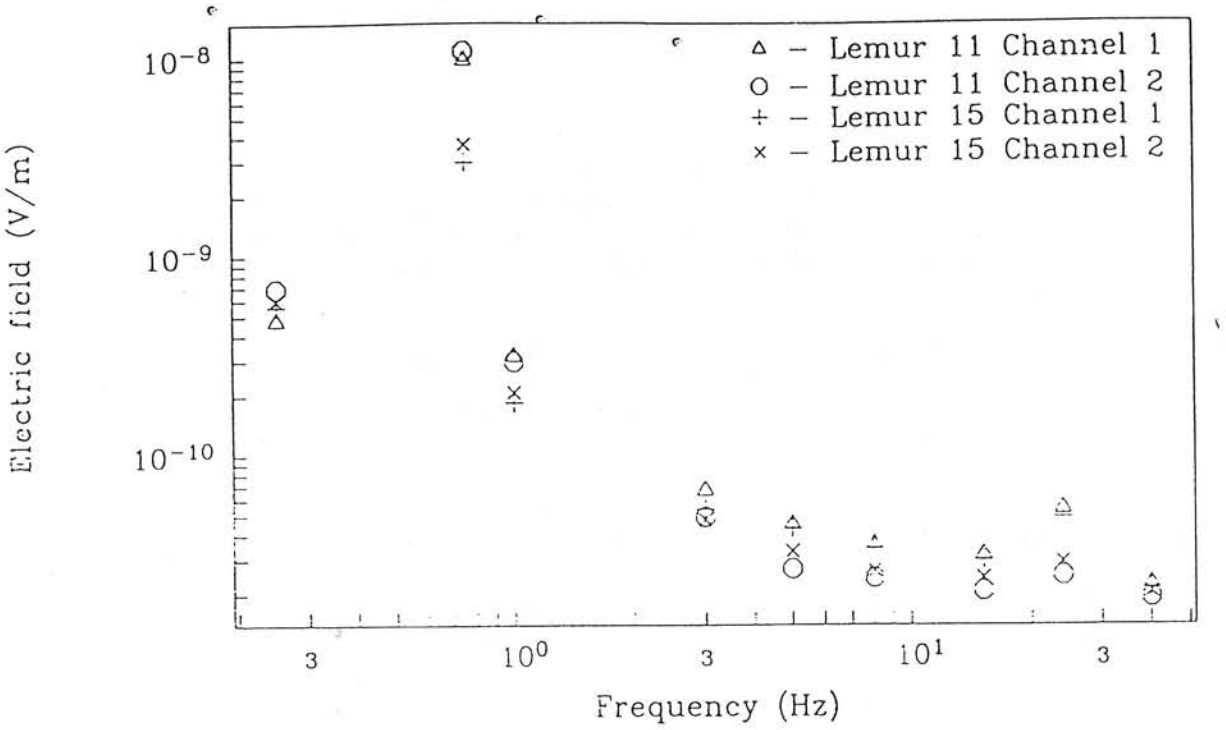

Figure 10. An amplitude spectrum of recorded noise, showing the amplitude in Vm^{-1} as a function of frequency. Channels 1 and 2 represent the two orthogonal components of horizontal electric field, measured by a total of 8 electrodes across two 13 m dipoles. The response of both channels and both instruments is similar, as expected. At frequencies above 3 Hz, the noise level is $<10^{-10}$ Vm^{-1}, and the spectrum is generally red, also as expected, due to the screening of externally generated fields by the water column. There is a pronounced peak in the spectrum at 0.75 to 1 Hz.

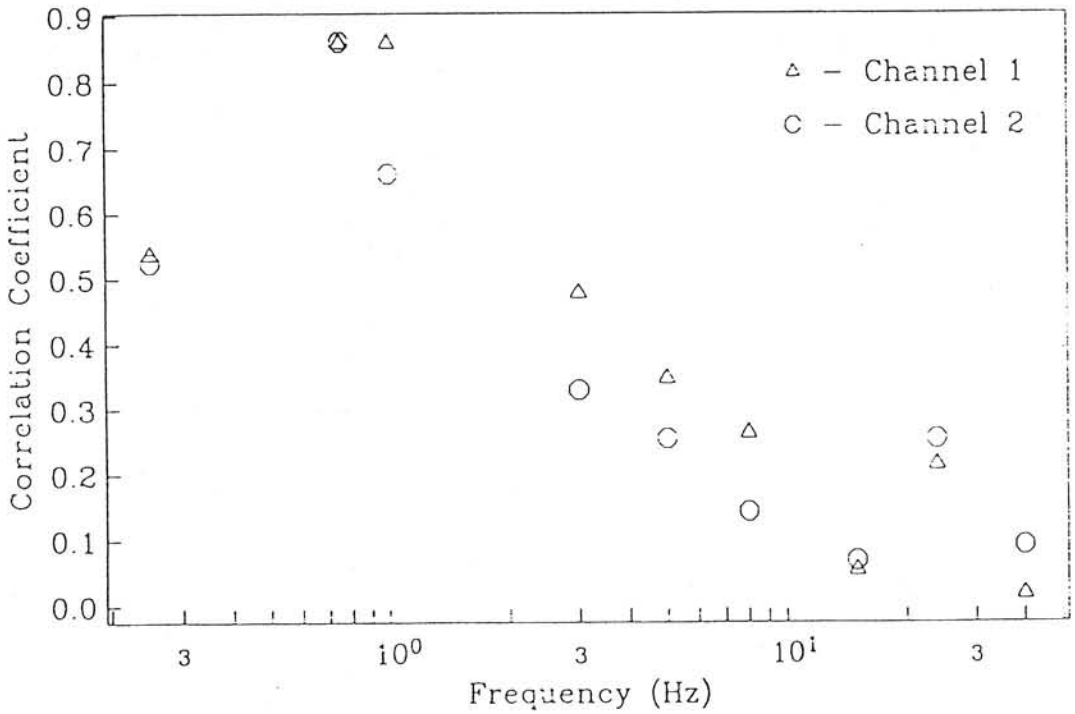

Figure 11. A plot of the coherence between the two independent recordings of each dipole made during the LEMUR test. It shows correlation coefficient (calculated from amplitudes only) as a function of frequency across the same frequency range as figure 10. At 0.75 to 1 Hz the noise spectrum is coherent between the two recordings, while at higher frequencies the coherence falls off sharply.

3. Cruise narrative

The duration of the cruise was 19 days and 9 hours. Of this, 9 days and 14 hours were spent on passage to and from Southampton to the work area, leaving a total of 9 days and 19 hours in the work area. Of the latter ~8 days 3 hours were spent shooting (although this period does include some downtime) and ~1 day 16 hours were spent on instrument deployment and recovery. A summary of the events that took place appears below. All turns were made at less than 4°/min. unless otherwise noted. All times are in GMT.

Wednesday 15th July (day 196)

10:40 Sailed from Southampton. Commenced passage to work area at maximum speed. Made good progress along the Channel due to favourable tidal conditions.

Thursday 16th July (day 197)

00:00 - 24:00 Continued passage to work area.

Friday 17th July (day 198)

00:00 - 24:00 Continued passage to work area.

Saturday 18th July (day 199)

00:00 Continued passage to work area.
14:00 Slowed to 8 knots to run up four compressors for airgun system initialisation.
16:00 Recommenced full steam passage to work area.

Sunday 19th July (day 200)

00:00 Continued passage to work area.
07:28 Heaved to float test LEMUR and deployed PES fish.
08:20 Continued full steam passage to work area.
14:00 Slowed to run up compressors.
16:00 Continued full steam passage to work area.

Monday 20th July (day 201)

06:55 Arrived at LEMUR deployment location.
07:25 LEMUR released, dunking transducer deployed.
09:17 LEMUR on seabed.
09:41 Recommencing passage to first seismic line location.
11:45 Head to wind at 3 knots and commencing deployment of streamer for balancing.
12:25 Tailbuoy deployed.
20:43 Streamer deployment complete. Airgun array deployment will commence at first light for health and safety reasons.

Tuesday 21st July (202)

06:00 Commencing airgun array deployment.
11:27 Airgun array deployment complete and test fired. Magnetometer deployed.
13:42 Slowed to less than 4 knots to add weight to front end of streamer.
14:18 MCS data acquisition system operational and triggering in sync with airgun firing system.
16:00 Heading to NW end of first MCS line (Line 34).
16:18 Commencing shot firing.
16 30 ***Start of Line 34.***
20:20 Deployed XBTs 1-3.
20:36 ***End of Line 34.***
21:36 ***Start of Line 31.***

Wednesday 22nd July (203)

01:30 ***End of Line 31.***
02:26 ***Start of Line 28.***
03:09 Sonobuoy A deployed.
06:00 ***End of Line 28.***
06:57 ***Start of Line 25.***
09:40 Deployed XBTs 4-5.
10:55 ***End of Line 25.***
11:44 ***Start of Line 22.***
15:15 ***End of Line 22.***
16:30 ***Start of Line 19.***
20:03 ***End of Line 19.***
20:57 ***Start of Line 16.***
21:52 Sonobuoy B deployed.

Thursday 23rd July (204)

00:49 ***End of Line 16.***
01:40 ***Start of Line 13.***
04:50 Electrical failure on ship's lighting system caused electrical power failure on compressor controller, shutting down compressors. Airgun array shut off before guns could flood and compressors restarted.
05:14 ***End of Line 13.***
05:41 Airguns firing again except for one of the 700 in^3 guns on the inner starboard array which has apparently flooded. Profile shooting order adjusted so that we shoot Line 35 in daylight tomorrow to enable airgun beam recovery and repair.
07:00 Starboard 700 in^3 airgun off.
07:04 ***Start of Line 10.***
11:00 ***End of Line 10.***
11:52 ***Start of Line 7.***
15:26 ***End of Line 7.***
16:00 Reftek problems.
16:39 ***Start of Line 4.***
21:00 ***End of Line 4.*** One of the starboard compressors failed and pressure relief valves blowing.
21:55 ***Start of Line 1.***
23:14 Starboard 300 in^3 gun turned off.

Friday 24th July (205)

01:59 ***End of Line 1.*** End of first pass through grid.
02:46 ***Start of Line 2.*** 11°/min. turn made onto this line by bridge.
05:20 Port 600 in^3 gun turned off.
06:56 ***End of Line 2.***
07:53 Recovering starboard airgun beams for repair and maintenance. Still firing port beams i.e. half the full array volume. Magnetometer recovered.
13:02 ***Start of Line 5.***
13:17 Sonobuoy C deployed.
13:30 Deployed XBT 6.
13:50 Deployed XBT 7.
18:05 Deployed starboard beams.
18:51 Outer starboard beam 120 in^3 gun not firing, recovered to effect further repair.
21:00 Airgun repair complete and starboard beams redeployed.
21:25 Magnetometer redeployed.

21:45 ***Start of Line 36.***
22:04 Compressor C problem. Firing rate dropped to 20 s and inner port beam guns (300, 600, 700 in^3) switched off to lower load. Nine guns only firing.
22:20 Emergency shutdown of all compressors.
22:48 Array firing at 20 s intervals. Eleven out of 12 guns operational. Port 600 in^3 gun switched off.
23:06 Firing rate increased to 15 s
23:06 Line 36 abandoned under advice of technical staff, who advised to shoot most important lines now as prospects for longevity of array and compressors not good.

Saturday 25th July (206)

00:00 ***Start of Line 37.***
04:34 ***End of Line 37.***
05:44 ***Start of Line 38.***
11:08 ***End of Line 38.***
12:03 Sonobuoy D deployed.
12:09 ***Start of Line 39.***
12:10 Sonobuoy E deployed.
12:35 Sonobuoy F deployed.
14:34 ***End of Line 39.***
15:25 ***Start of Line 15.***
18:35 ***End of Line 15.***
18:54 ***Start of Line 20.***
22:54 ***End of Line 20.***

Sunday 26th July (207)

00:00 ***Start of Line 17.***
03:30 ***End of Line 17.***
04:15 ***Start of Line 14.***
08:15 ***End of Line 14.***
09:11 ***Start of Line 18.***
12:38 ***End of Line 18.***
13:45 ***Start of Line 21.***
17:20 ***End of Line 21.***
18:20 ***Start of Line 24.***
20:24 Starboard 600 in^3 gun turned off.
21:45 ***End of Line 24.***
22:46 ***Start of Line 27.***

Monday 27th July (208)

02:19 ***End of Line 27.***
03:16 ***Start of Line 30.***
07:03 ***End of Line 30.***
08:00 ***Start of Line 32.***
11:39 ***End of Line 32.***
12:06 Sonobuoy G deployed.
12:58 ***Start of Line 29.***
15:23 Compressor problems. Compressor A shutdown. Two compressors remaining, both 600 in^3 guns switched off.
16:28 ***End of Line 29.***
17:06 Sonobuoy H deployed.
17:34 ***Start of Line 26.***
17:38 All guns turned off.
17:54 All ten remaining functional guns back on.
20:57 ***End of Line 26.***
22:05 ***Start of Line 23.***

Tuesday 28th July (209)

01:39 ***End of Line 23.***
02:45 Starboard 700 in^3 gun turned off.
04:17 ***Start of Line 12.***
07:50 ***End of Line 12.***
08:50 ***Start of Line 8.***
11:42 Sonobuoy I deployed.
12:14 ***End of Line 8.***
13:57 ***Start of Line 36/2*** (shooting of remaining part of Line 36 not already shot).
18:22 ***End of Line 36/2.***
20:33 ***Start of line 39/2*** (shooting of remaining part of Line 39 not already shot).

Wednesday 29th July (210)

00:33 ***End of Line 39/2.***
00:53 ***Start of Line 6/1.*** (Line to be shot in two parts to optimise remaining ship time and minimise turns).
01:50 ***End of Line 6/1.***
03:15 ***Start of Line 3.***
06:31 ***End of Line 3.***
07:45 ***Start of Line 6/2.***
09:01 Firing rate dropped to 20 s. Remaining two compressors can't handle the load.
10:44 ***End of Line 6/2.***
12:20 ***Start of Line 11.***
15:18 ***End of Line 11.***
16:50 ***Start of Line 35.***
17:10 Port 466 in^3 gun turned off. Eight firing guns remaining.
19:10 ***End of Line 35.*** End of seismic profiling.
19:15 Noise test on system completed.
20:20 Magnetometer recovered. Commencing airgun array recovery.
20:50 Recovery of airgun array completed. Commencing streamer recovery.
23:50 Recovery of streamer completed.

Thursday 30th July (211)

00:06 XBT 8 deployed.
00:17 XBT 9 deployed.
01:00 XBT 10 deployed.
01:11 XBT 11 deployed.
01:20 XBT 12 deployed.
01:27 XBT 13 deployed.
01:36 XBT 14 deployed.
01:44 XBT 15 deployed.
01:45 - 04:14 XBTs 16-24 deployed. Steaming to LEMUR deployment position.
05:20 On station at LEMUR deployment site and commencing recovery.
07:05 LEMUR on surface.
07:28 LEMUR on board.
07:36 Commencing passage to Southampton.

Friday 31st July (212)

00:00 - 24:00 Continued passage to Southampton.

Saturday 1st August (213)

00:00 - 24:00 Continued passage to Southampton.

Sunday 2nd August (214)

00:00 - 24:00 Continued passage to Southampton.

Monday 3rd August (215)

20:00 Arrive Southampton. End of cruise D235c.

4. Equipment performance

This cruise was marred by considerable equipment failure which stemmed largely from a number of factors related to pre-cruise preparation. The bulk of the failure can be attributed to some component of the compressor system, or installation of ship's equipment in conjunction with this system, combined with ill-timed pre-cruise preparation. We experienced no bad weather throughout the duration of this cruise.

4.1 Seismic experiment

4.1.1 Multichannel seismic experiment

Onboard data quality control and processing

We installed a small network of UNIX workstations, a PC and a postscript laser printer in the main lab to undertake underway quality control and basic processing of the acquired data. Two of the UNIX workstations had a version of ProMAX installed to facilitate this processing. The quality control process included: a) investigation of bad traces; b) analysis of overall noise content; and c) frequency analysis such that the need for any streamer or airgun array maintenance could be identified (see figure 12).

In addition to the quality control we also performed a degree of basic processing. An example of the results of this processing are shown in figure 8.

Airgun array

Prior to the cruise a considerable period of time was spent modelling both the array configuration and its towing depth, to optimise the source signature for the requirements of the target of this investigation. During the cruise we experienced two main problems associated with the airgun array. The first, the repeated loss of the bigger guns after a relatively short period of time, the second was the lack of control over the towing depths of the airgun beams. In this kind of work it is important to be able to tow both the source of seismic energy and the receivers consistently at a certain depth below the surface. Our experiment was designed around an airgun array towing at a depth of 8 m and a streamer towing at a depth of 12 m - neither of which were we able to achieve despite the best efforts of the technical staff. Taking into account that the guns themselves hang at about 1m below the beams, and that the floats do not tow directly above their attachment point but somewhere between 30 and 40° aft; to achieve 8 m towing depth a rope length of between 10 and 14 m would be required. Thus a 12 m length seemed an ideal compromise. However, on deployment a depth of more than 15 m was measured by both depth sensors each beam. Thus assuming that the floats tow immediately above the attachment point (i.e. the shortest rope path) the rope must have either stretched by at least 25% and more likely by 75%, using the assumption that the floats tow behind the attachment point. The alternative explanation may be that all 8 depth sensors were inaccurate or incorrectly calibrated. To us the former seems more likely, as all depth sensors were checked, recalibrated and found to be functioning perfectly on recovery. So this begs the question - why use rope that stretches by this amount? This situation effectively gave us no control over the seismic source signature, something crucial to data quality and subsequent data processing. Recovery, shortening of each of the four ropes and redeployment would have taken ~24 hours - about 1/8th of the total shot firing period. For this cruise the suspension ropes used were constructed from cheap polypropylene - totally unsuitable for this task. Non-stretching kevlar (or such like) suspension ropes would have been more appropriate for this task. A prime example of a relatively minor cost saving exercise that severely degraded the scientific capability of the cruise.

In the many years of experience of both PIs of seismic acquisition using airgun arrays, the biggest guns in the array are found to be the most reliable. The repeated loss of the bigger guns in the array after short periods of time represented an extremely high attrition rate, such that if we had to repair every failure, we would have spent about half of the shot firing period undertaking maintenance. This level of downtime was not realistic in relation to the actual length of the shot firing period, and thus the underway quality control was used to monitor when repair and maintenance of the array was absolutely necessary in relation to the degrading source signature. The effect of the progressive loss of airguns on the source signature is shown in figure 12. The length of time required to undertake maintenance on the larger guns is exacerbated by the way the array is constructed of a number of beams, each having three guns. The optimum source array required the larger guns to be located on the

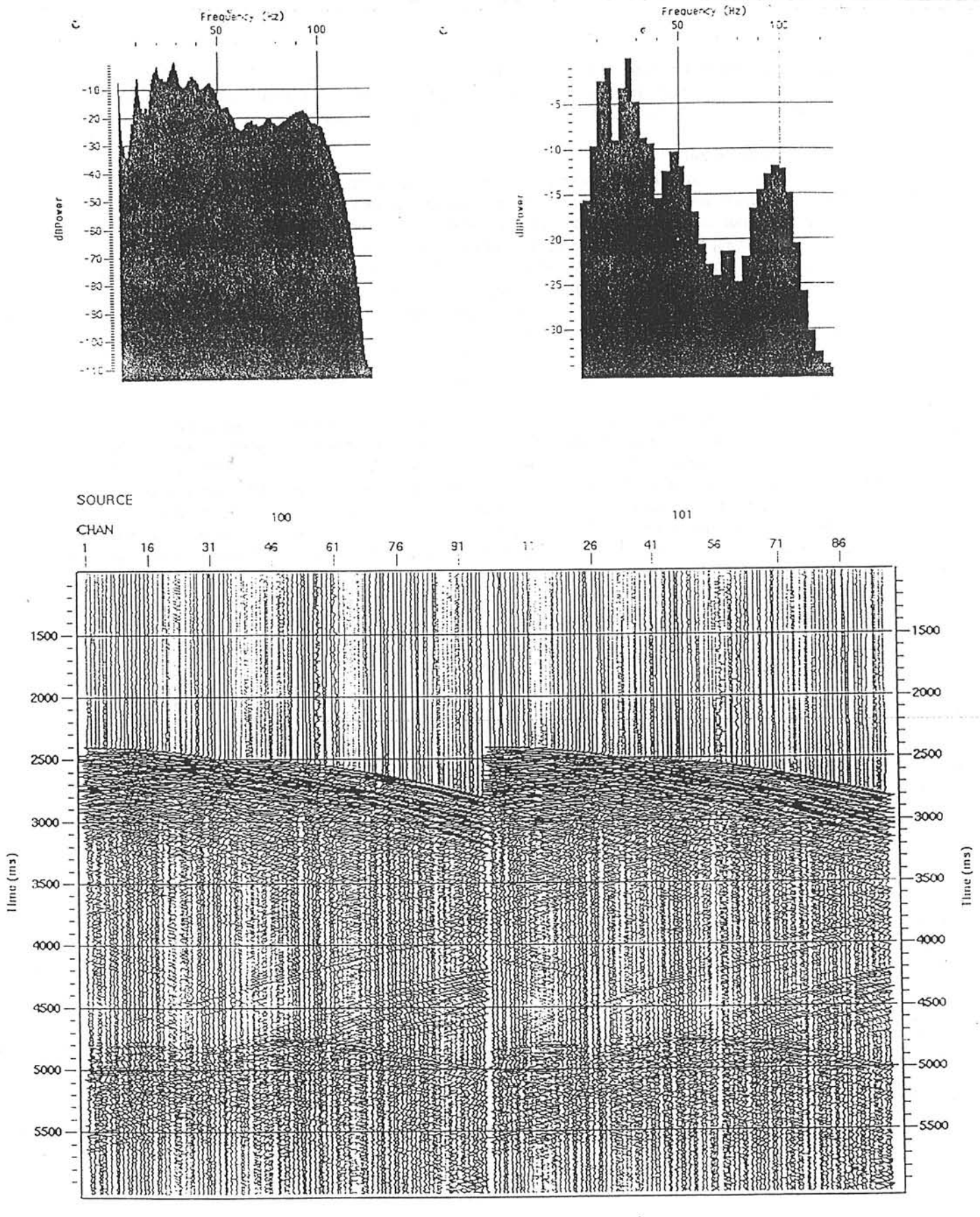

Figure 12. Example gathers and frequency analysis of the seismic data collected during D235c. UPPER: frequency spectrum of data post (left) and pre (right) array maintenance and repair. Note the large notch in the frequency spectrum related to the loss of a number of the guns in the array. LOWER: two shot point gathers showing the raw data. Note the noisy trace - channel 57.

inner two beams. To maintain the inner beams the outer beams also need to be recovered. Thus to save time the array was maintained in two stages, one half at a time, such that acquisition could still continue by firing one half of the array while maintaining the other half.

Multichannel streamer

The 2.4 km Teledyne analogue streamer performed reasonably well considering its age. However, difficulties were experienced in maintaining the planned towing depth and a level streamer, the latter compounded to some extent by current and wind directions relative to the profile orientations. Only one channel, 57, showed persistent noise problems throughout surveying, while channels 47 and 61 became progressively noisier as shooting progressed, see figure 12. During one turn, see later, the streamer sank quite deep, although the exact depth was difficult to ascertain as a number of the depth sensors appeared to be giving spurious readings. This incident probably triggered three of the retrievers to inflate, although these appeared to have no effect on the towing depth or geometry of the streamer. The inflated retrievers were the only damage experienced to the streamer.

Compressors

Despite repeated requests and 12 months notice, the shipboard compressors were not completely rebuilt and certificated until just a day before the cruise was due to start. Thus they were not run for any length of time either loaded or unloaded. In addition the containerised backup compressors were not supplied for this cruise due to financial reasons within RVS, although they were "promised", after discussion of the air requirements and the potential reliability of the onboard compressors after their rebuild, at the cruise planning meeting. It is therefore unsurprising that two of the compressors lasted a mere 96 and 125 hours respectively before major part failure for which there were limited, or no, spares. Further progressive failure occurred which resulted in one failed compressor being used for spares and, ultimately, in an increase in the firing period from 15 to 20 s as the remaining two compressors (one of which was loosing 7 litres of oil per day) could not handle the load. If the array volume had not been downsized prior to the cruise and if we had not already lost 3 out of 4 of the biggest guns it would not have been possible to achieve a firing solution.

Multichannel seismic acquisition system

The newly purchased Geometrics 96-channel acquisition system functioned without fault, greatly assisted in its first use by technical support from a contractor.

Turns

At the planning meeting for this cruise it was agreed that, in good weather, a turning rate of 4°/min was the maximum advisable with the towing configuration of the airgun array and streamer. However, during the cruise one turn towards the northern end of the survey area was conducted significantly above this rate (~11°/min) despite written and verbal notification of its existence (and a suggested approach to its execution) by both PIs and the Master, causing the streamer to sink quite deeply (and probably causing most of the damage to its component parts) and which could have potentially caused a major tangle of the airgun array with the streamer.

However, it should be noted that the requested turn rate of 4°/min caused no surveying or equipment problems.

4.1.2 Sonobuoy deployments

No sonobuoy deployments were successful during this cruise largely due to entanglement or collision with the towed seismic equipment. This problem is largely due to the lack of sonobuoy deployment system, other than dropping them over the side by hand, on NERC' ships.

4.2 LEMUR test

As noted in Section 2.3 the LEMUR deployment was completely successful, with both instruments recovered having recorded data according to their programming.

4.3 XBTs

Similar deployment problems were experienced with the XBTs to the sonobuoys although 20 out of 29 deployments were successful, largely because they were deployed post-recovery of the seismic acquisition system. See Table 5. However, floppy disk drive failure on the acquisition PC did result in the loss of some data.

4.4 Other scientific equipment

Other scientific equipment functioned largely without fault, although some underway repair/maintenance was required on the PES fish deployment system and its onboard connections.

4.5 Ship's machinery and fitted equipment

Ship's equipment failures were as follows:

a) Steering gear in port	-	40 minutes and further delay in sailing
b) Loss of electrical supply to the compressors related to an electrical failure of lighting in the galley	-	10 minutes loss in electrical power which resulted in 1 hour or 9 km of line being unshot due to compressor shut down and system reinitiation

The latter of these failures had the potential of flooding of the entire airgun array were it not for the swift action of a technician hired by RVS for this cruise. Potential downtime for an incident of this kind would be of the order of about 24-36 hours for complete recovery, strip down, rebuild and redeployment of the array - about 13-20% of the total surveying time in this case.

5. Other factors affecting cruise outcome

Effectiveness of cruise planning procedures

Efficient and effective cruise planning revolves around direct and uncorrupted communication between all parties concerned. The whole point of a cruise planning meeting is to clarify customer requirements and agree, based on the available equipment base and expertise, what is necessary to conduct a viable scientific cruise. Once agreement is reached all parties should keep each other informed if circumstances change, no matter how apparently minor, throughout the entire period until sailing. This clearly did not happen with this cruise. The level of communication between RVS and the end user was very poor, particularly concerning major equipment and staff problems, which could have had major consequences for the viability of this cruise or it taking place at all. We recommend that a cruise liaison officer, or more importantly one with a technical background, should be appointed for each cruise and be required to assimilate information from all equipment groups within RVS and pass this on in report form at least once a week until the cruise takes place. This role should also be bi-directional, with the liaison officer passing on information from the Principal Scientist(s) back to the equipment groups.

In the current scheme of things there appears to be a major blockage somewhere between the "people on the ground" who prepare, mobilise and operate equipment for a cruise and the Principal Scientist(s) who has specific requirements for valid scientific reasons.

Mobilisation/Demobilisation days vs. sailing days

Another aspect of communication between the PI(s) and Operations and Planning that really needs addressing is a clear, documented outline of what exactly is meant by the departure and arrival days. Ideally this should be included with the ship time application forms, together with a statement of how many mob. and demob. days are required for particular types of cruises. In this particular case we were told at the last minute that we would sail "early afternoon" on our departure day (effectively losing 6 hrs of science time) and must arrive by 8 am on our arrival day (effectively losing 24 hrs of science time), with mob. and demob. already included on either side. If an 8 am arrival is always the case on an arrival day then that day should be termed a demob. day as that is what it effectively is in reality. Mobilisation requirements for the main cruise types should be outlined on the ship time application form for planning purposes in addition to nominal sailing and arrival times.

Equipment longevity and readiness

It has become perfectly obvious both prior to and during this cruise that RVS is in financial crisis and that staff morale is extremely low. It became apparent during mobilisation that the majority of the most fundamental equipment to be used during this cruise was nowhere near ready and that this was largely due to a lack of finances and man-power, with the man-power problem stemming in part from a large number of staff on sick leave or having resigned.

From the point of view of the science, the lack of a complete and reliable set of onboard compressors necessitated an underway major reappraisal and redesign of the scientific programme, largely because of an extreme lack of confidence that things would last much longer than they already had. Ultimately a change in firing rate from the optimum requested resulted, simply because the two remaining functional compressors couldn't handle the load, even with three of the biggest guns not operational. In addition, the majority of the larger guns in the array (usually the most reliable) failed within a short period of being deployed, and failed again within a short period of being recovered, serviced and redeployed. This was a fairly short cruise, with only ~8 days of actual array firing. In that time we lost 2 compressors and the majority of the bigger guns in the array. In addition, the first compressor to die began to be used for spares to keep the remainder going. A summary of the cruise statistics is shown in Table 6.

We have come to the conclusion that, as it stands, RVS is for a number of reasons probably no longer capable of supporting a full length airgunning cruise using a reasonable volume airgun array and a firing rate suitable for multichannel work, without significant investment in their equipment base. In addition RVS probably no longer has sufficient, experienced staff to prepare or maintain the equipment let alone operate it at sea. It has become perfectly clear to us that too much has been expected of both the non-sailing and sailing technical staff, and that only their professionalism, goodwill and pride in their jobs has enabled this cruise to take place and data to be acquired. To these people we owe a great deal and words alone cannot express our gratitude. We also wish to take this opportunity to state that we feel that it is totally unacceptable to expect these people to work under these conditions. It is not surprising that so many staff simply cannot cope with the stress that this kind of working practise undoubtedly heaps upon their shoulders. Experience of equipment use and repair at sea is a priceless commodity, not quickly or easily learned - once it is gone it is gone forever.

6. Conclusions

Multichannel seismic data acquisition occurred during this cruise despite numerous technical difficulties, mostly revolving around the installation and commissioning of the onboard compressors. Despite this 37 normal incidence seismic profiles were acquired over three across-axis and 1 along-axis passes of the 57° 45' AVR and adjacent AVR-tips although none of these profiles were acquired with the requested parameters.

This cruise has shown that the RVS deployed seismic acquisition equipment is long overdue for financial investment or, better still, replacement.

Finally, this cruise would not have taken place at all if it were not for the truly professional attitude of the "people on the ground" who actually prepare the equipment for sea and those that have to "make the best of it" when it is deployed at sea. RVS should pride themselves in having such staff and make every effort to keep them, support them with new staff and financially support proper and adequate maintenance and pre-cruise preparation programmes, including investing in new equipment and adequate spares for the entire equipment base, and starting a technical liaison officer scheme from the day the ship time is first awarded.

Acknowledgements

We wish to thank the master, officers and crew of the *RRS Discovery* and the support staff and sea-going technicians of NERC's Research Vessel Services for their efforts throughout this cruise. We would also like to thank Sean Young from Geometrics whose assistance on all matters seismic was also greatly appreciated. This work was funded by the University of Durham and the U.K.'s Natural Environment Research Council through their BRIDGE programme, who also supported data processing and interpretation through a research grant (BRIDGE 105).

References

Burnett, M.S., Caress, D.W. & Orcutt, J.A. (1989). Tomographic image of the ..... Nature, 339, 206-208.

Calvert A., 1995, Seismic evidence for a magma chamber beneath the slow-spreading Mid-Atlantic Ridge, Nature, 377, 410-414.

Charlou, J.L., Rona, P. and Bougault, H. (1987). Methane anomalies over TAG ..... J. Mar. Res., 45, 461-472.

Collier, J. & Sinha, M. (1990). Seismic images of a magma chamber beneath the Lau Basin ..... Nature, 346, 646-648.

Collier, J.S. & Sinha, M.C., 1992. The Valu Fa Ridge: the pattern of volcanic activity ..... Marine Geology, 104, 243 - 263.

Collier, J.S. & Sinha, M.C., 1992. Seismic mapping of a magma chamber ..... J. Geophys. Res., 97, 14,031 - 14,053.

Detrick, R.S., Buhl, P., Vera, E., Mutter, J., Orcutt, J., Madsen, J. & Brocher, T. (1987). Multi-channel seismic imaging of a crustal magma chamber along the East Pacific Rise. Nature, 326, 35-42.

Detrick, R.S., Mutter, J.C., Buhl, P. & Kif, I.I. (1990). No evidence from multichannel ..... Nature, 347, 61-64.

Detrick, R. S., Harding, A. J., Kent, G. M., Orcutt, J. A., Mutter, J. C. and Buhl, P. (1993). Seismic structure of the southern East Pacific Rise. Science, 259, 499-503.

Garmany, J. (1989), Accumulations of melt at the base of young oceanic crust. Nature, 340, 628-632.

Harding, A.J., Orcutt, J.A., Kappus, M.E., Vera, E.E., Mutter, J.C., Buhl, P., Detrick, R.S & Brocher, T.M. (1989). The structure of young oceanic crust at 13oN on the East pacific Rise ..... J. Geophys. Res., 94, 12,163-12,196.

Kent, G.M., Harding, A.J. & Orcutt, J.A. (1990). Evidence for a smaller magma chamber ..... Nature, 344, 650-653.

Kent, G. M., Harding, A. J., & Orcutt, J. A., 1993a. Distribution of magma beneath the East Pacific Rise between the Clipperton Transform and the 9 17' N Deval from forward modelling of common depth point data. J. Geophys. Res. 98, 13945-13969.

Kent, G. M., Harding, A. J., & Orcutt, J. A., 1993b. Distribution of magma beneath the East Pacific Rise near the 9 03' N overlapping spreading centre from forward modelling of common depth point data. J. Geophys. Res. 98, 13971-13995.

Kusznir, N.J. & Bott, M.H.P. (1976). A thermal study of the formation of oceanic crust. Geophys. J. Roy. astr. Soc., 47, 83-95.

Langmuir, C.H., Bender, J.F. & Batiza, R. (1986). Petrologic and tectonic segmentation ..... Nature , 322, 422-429.

Macdonald, K.C., K.C., Miller, S.P., Luyendyk, B.P., Atwater, T.M. and Shure, L. (1983). Investigation of a Vine-Matthews magnetic lineation from a submersible: the source and character of marine magnetic anomalies. J. Geophys. Res., 88, 3403-3418.

Macdonald, K.C., Sempere, J.C. & Fox, P.J. (1984). East Pacific Rise from ..... J. Geophys. Res., 89, 6049-6069.

MacGregor, L.M., Sinha, M.C. and Constable, S., 1998, The RAMESSES experiment - III. Controlled-source electromagnetic sounding of the Reykjanes Ridges at 57° 45'N, G. J. Int., 135, 773-789.

Murton, B. J. & Parson, L. M. (1993). Segmentation, volcanism and deformation of oblique ..... Tectonophysics.

Navin D.A., Peirce, C. and Sinha, M.C., 1998, The RAMESSES experiment - II. Evidence for accumulated melt beneath a slow spreading ridge from wide-angle refraction and multichannel reflection seismic profiles, G. J. Int., 135, 746-772.

Parson, L. M. et al. (1993). En echelon axial volcanic ridges at the Reykjanes Ridge: ..... Submitted to Earth Planet. Sci. Lett.

Searle, R.C. and Laughton, A.S. (1981). Fine-scale sonar study of tectonics .... the Reykjanes Ridge. Oceanologica Acta, 4, 5-13.

Searle, R.C., Field, P.R. and Owens, R.B. (1994). Segmentation and a non-transform ..... J. Geophys. Res., 99, 24159-24172.

Sinha, M.C., Navin, D.A., MacGregor, L.M., Constable, S., Peirce, C., White A., Heinson, G. and Inglis M.A., 1997, Evidence for accumulated melt beneath the slow-spreading Mid-Atlantic Ridge, Phil. Trans. R. Soc. Lond. A, 355, 233-253.

Sinha, M.C., Constable, S.C., Peirce, C., White, A., Heinson, G., MacGregor, L.M. and Navin, D.A., 1998, Magmatic processes at slow spreading ridges: implications of the RAMESSES experiment at 57° 45'N on the Mid-Atlantic Ridge, G. J. Int., 135, 731-745.

Sleep, N.H. (1975). Formation of oceanic crust - some thermal constraints. J. Geophys. Res., 80, 4037-4042.

Tivey, M. A. and H. P. Johnson (1987). The central anomaly magnetic high: Implications for ocean crust construction and evolution. J. Geophys. Res. 92, 12,685-12,694.

Toomey D.R., Purdy G.M., Solomon S.C. & Wilcock W.S.D. (1990). The three-dimensional seismic velocity structure of the East Pacific Rise near 9o30'N. Nature, 347, 639-645.

Vera, E.E., Mutter, J.C., Buhl, P., Orcutt, J.A., Harding, A.J., Kappus, M.E., Detrick, R.S. & Brocher, T.M. (1990). Structure of 0- to 0.2-m.y. old oceanic crust at 9°N on the East Pacific Rise from expanded spread profiles. J. Geophys. Res., 95, 15529-15556.

Table 1
Scientific personnel

Dr C. Peirce (PI/PSO)	University of Durham
Dr M.C. Sinha (Co PI)	University of Cambridge
Mr I.M. Turner	University of Durham
Mr A.J. Day	University of Durham
Mr D.M.D. Davies	University of Durham
Miss J.R.L. Brett	University of Durham
Dr L.M. MacGregor	University of Cambridge
Mr S. Topping	University of Cambridge
Mr D. Shewan	University of Cambridge
Miss L. Hall	University of Cambridge
Mr C. Day	RVS
Mr D. Dunster	RVS
Mr D. Rees	RVS
Mr C. Paulson	RVS
Mr D. Booth	RVS
Mr I. Udal	RVS
Mr G. Knight	RVS
Mr S. Young	Geometrics
Mr A. Cumming	Ex RVS (contracted in especially for this cruise)
Capt. R.C. Plumley and staff	RVS Marine

Table 2
LEMUR deployment

Deployment position:	
Latitude	57° 25.39' North
Longitude	31° 35.80' West
Water depth	2674 m
Deployment:	
date/time released	20/07/98 07:24:35 Z
date/time reached bottom	20/07/98 09:05:00 Z
descent rate	26.6 m/min.
Recovery:	
date/time released	30/07/98 05:45 Z
date/time surfaced	30/07/98 07:05 Z
ascent rate	33.4 m/min.
Data recorded:	
Instrument 11	340 MBytes
Instrument 15	340 MBytes

Table 3
Planned multichannel seismic profile locations

Multichannel Seismic Line Locations - version 1

Way points	From					To					Way points
	Line	Lat N		Long E		Lat N		Long E		Line	
WP25	1	58.056	58 03.351	327.241	32 45.560	57.886	57 53.162	327.835	32 09.915	1	WP24
WP59	2	58.044	58 02.649	327.229	32 46.272	57.874	57 52.432	327.823	32 10.602	2	WP60
WP58	3	58.032	58 01.919	327.217	32 46.983	57.862	57 51.730	327.811	32 11.340	3	WP57
WP22	4	58.020	58 01.216	327.205	32 47.695	57.850	57 50.973	327.800	32 12.000	4	WP23
WP62	5	58.008	58 00.486	327.193	32 48.408	57.838	57 50.297	327.786	32 12.815	5	WP61
WP55	6	57.996	57 59.784	327.181	32 49.120	57.827	57 49.595	327.775	32 13.527	6	WP56
WP21	7	57.985	57 59.100	327.167	32 49.980	57.816	57 48.960	327.760	32 14.400	7	WP20
WP63	8	57.973	57 58.380	327.156	32 50.640	57.804	57 48.240	327.750	32 15.000	8	WP64
WP54	9	57.962	57 57.720	327.144	32 51.360	57.792	57 47.520	327.738	32 15.720	9	WP53
WP18	10	57.950	57 57.000	327.133	32 52.020	57.780	57 46.800	327.725	32 16.500	10	WP19
WP66	11	57.937	57 56.220	327.119	32 52.860	57.768	57 46.080	327.714	32 17.160	11	WP65
WP51	12	57.926	57 55.560	327.107	32 53.580	57.756	57 45.360	327.701	32 17.940	12	WP52
WP17	13	57.914	57 54.840	327.095	32 54.300	57.744	57 44.640	327.689	32 18.660	13	WP16
WP67	14	57.902	57 54.120	327.083	32 55.020	57.732	57 43.946	327.676	32 19.425	14	WP68
WP50	15	57.890	57 53.400	327.073	32 55.620	57.721	57 43.260	327.667	32 19.980	15	WP49
WP14	16	57.878	57 52.680	327.061	32 56.340	57.709	57 42.540	327.655	32 20.700	16	WP15
WP70	17	57.866	57 51.960	327.048	32 57.120	57.696	57 41.760	327.641	32 21.540	17	WP69
WP47	18	57.855	57 51.300	327.037	32 57.780	57.685	57 41.100	327.629	32 22.260	18	WP48
WP13	19	57.842	57 50.520	327.024	32 58.560	57.673	57 40.380	327.616	32 23.040	19	WP12
WP79	20	57.873	57 52.380	326.862	33 08.280	57.450	57 27.000	328.343	31 39.450	20	WP80
WP46	21	57.819	57 49.140	327.000	33 00.000	57.650	57 39.000	327.592	32 24.480	21	WP45
WP10	22	57.807	57 48.420	326.989	33 00.660	57.638	57 38.280	327.580	32 25.200	22	WP11
WP71	23	57.795	57 47.700	326.969	33 01.860	57.626	57 37.560	327.568	32 25.920	23	WP72

WP43	24	57.783	57 46.980	326.964	33 02.010	57.614	57 36.840	327.556	32 26.640	24	WP44
WP9	25	57.772	57 46.320	326.954	33 02.760	57.602	57 36.120	327.542	32 27.480	25	WP8
WP74	26	57.759	57 45.540	326.940	33 03.600	57.591	57 35.460	327.532	32 28.080	26	WP73
WP42	27	57.747	57 44.820	326.929	33 04.260	57.578	57 34.680	327.520	32 28.800	27	WP41
WP6	28	57.736	57 44.160	326.917	33 04.980	57.567	57 34.020	327.509	32 29.460	28	WP7
WP75	29	57.724	57 43.440	326.905	33 05.420	57.554	57 33.240	327.497	32 30.180	29	WP76
WP39	30	57.712	57 42.720	326.893	33 06.420	57.542	57 32.520	327.486	32 30.840	30	WP40
WP5	31	57.700	57 42.000	326.881	33 07.140	57.531	57 31.860	327.473	32 31.620	31	WP4
WP78	32	57.688	57 41.280	326.871	33 07.740	57.519	57 31.140	327.461	32 32.340	32	WP77
WP38	33	57.676	57 40.560	326.857	33 08.580	57.507	57 30.420	327.449	32 33.060	33	WP37
WP2	34	57.664	57 39.840	326.845	33 09.300	57.494	57 29.640	327.437	32 33.780	34	WP3
WP26	35	58.054	58 03.230	327.251	32 44.949	57.597	57 35.820	327.083	32 55.020	35	WP27
WP29	36	58.031	58 01.838	327.332	32 40.068	57.575	57 34.500	327.161	32 50.340	36	WP28
WP30	37	58.010	58 00.568	327.408	32 35.492	57.552	57 33.120	327.240	32 45.600	37	WP31
WP33	38	57.987	57 59.243	327.485	32 30.915	57.530	57 31.800	327.317	32 40.980	38	WP32
WP34 WP35	39	58.000 via 57.701	58 00.000 57 42.060	327.609 327.466	32 23.442 32 32.060	57.508	57 30.480	327.395	32 36.300	39	WP36

Shooting order / line	Heading/shooting direction	Comments
34	SE	
31	NW	
28	SE	Sonobuoy A
25	NW	
22	SE	
19	NW	
16	SE	Sonobuoy B
13	NW	
10	SE	
7	NW	
4	SE	
1	NW	
35	S	
36	N	Sonobuoy C, D, E
37	S	Sonobuoy F, G
38	N	Sonobuoy H, I
39	S	Sonobuoy J, K, L
33	NW	
30	SE	
27	NW	
24	SE	
21	NW	
18	SE	
15	NW	
12	SE	
9	NW	Sonobuoy M
6	SE	
3	NW	Fish tail to line 2 *
2	SE	
5	NW	
8	SE	
11	NW	
14	SE	
17	NW	
23	SE	
26	NW	Sonobuoy N
29	SE	
32	NW	
20	SE	

* Note this turn requires *light bulbing* or *fish tailing* as is tighter than 4°/min.

Table 4
Actual multichannel seismic profile locations

Multichannel Seismic Line Locations -version 6

Way points	From					To					Way points
	Line	Lat N		Long E	Long W	Lat N		Long E	Long W	Line	
WP25	1	58.056	58 03.351	327.241	32 45.540	57.904	57 54.240	327.775	32 13.500	1	WP24
WP59	2	58.044	58 02.649	327.229	32 46.260	57.891	57 53.460	327.763	32 14.220	2	WP60
WP58	3	58.032	58 01.919	327.217	32 46.980	57.880	57 52.800	327.749	32 15.060	3	WP57
WP22	4	58.020	58 01.216	327.205	32 47.700	57.868	57 52.080	327.737	32 15.780	4	WP23
WP62	5	58.008	58 00.486	327.193	32 48.420	57.856	57 51.360	327.725	32 16.500	5	WP61
WP55	6	57.996	57 59.784	327.181	32 49.140	57.845	57 50.700	327.714	32 17.160	6	WP56
WP21	7	57.976	57 58.560	327.200	32 48.000	57.833	57 49.980	327.702	32 17.880	7	WP20
WP63	8	57.965	57 57.900	327.188	32 48.720	57.821	57 49.260	327.690	32 18.600	8	WP64
WP54	9	57.953	57 57.180	327.176	32 49.440	57.809	57 48.540	327.678	32 19.320	9	WP53
WP18	10	57.941	57 56.460	327.164	32 50.160	57.797	57 47.820	327.666	32 20.040	10	WP19
WP66	11	57.928	57 55.680	327.151	32 50.940	57.786	57 47.160	327.653	32 20.820	11	WP65
WP51	12	57.917	57 55.020	327.139	32 51.660	57.773	57 46.380	327.641	32 21.540	12	WP52
WP17	13	57.905	57 54.300	327.127	32 52.380	57.761	57 45.660	327.629	32 22.260	13	WP16
WP67	14	57.893	57 53.580	327.115	32 53.100	57.750	57 45.000	327.617	32 22.980	14	WP68
WP50	15	57.881	57 52.860	327.103	32 53.820	57.739	57 44.340	327.606	32 23.640	15	WP49
WP14	16	57.869	57 52.140	327.092	32 54.480	57.727	57 43.620	327.594	32 24.360	16	WP15
WP70	17	57.857	57 51.420	327.080	32 55.200	57.714	57 42.840	327.581	32 25.140	17	WP69
WP47	18	57.846	57 50.760	327.068	32 55.920	57.703	57 42.180	327.570	32 25.800	18	WP48
WP13	19	57.833	57 49.980	327.054	32 56.760	57.690	57 41.400	327.556	32 26.640	19	WP12
WP79	20	57.873	57 52.380	326.862	33 08.280	57.573	57 34.380	327.904	32 05.760	20	WP80
WP46	21	57.802	57 48.120	327.061	32 56.340	57.659	57 39.540	327.561	32 26.340	21	WP45
WP10	22	57.790	57 47.400	327.051	32 56.940	57.647	57 38.820	327.550	32 27.000	22	WP11
WP71	23	57.777	57 46.620	327.036	32 57.840	57.635	57 38.100	327.538	32 27.720	23	WP72
WP43	24	57.766	57 45.960	327.025	32 58.500	57.623	57 37.380	327.525	32 28.500	24	WP44

WP9	25	57.755	57 45.300	327.014	32 59.160	57.610	57 36.600	327.513	32 29.220	25	WP8
WP74	26	57.742	57 44.520	327.000	33 00.000	57.599	57 35.940	327.503	32 29.820	26	WP73
WP42	27	57.730	57 43.800	326.990	33 00.600	57.586	57 35.160	327.490	32 30.600	27	WP41
WP6	28	57.719	57 43.140	326.978	33 01.320	57.576	57 34.560	327.479	32 31.260	28	WP7
WP75	29	57.706	57 42.360	326.966	33 02.040	57.563	57 33.780	327.446	32 33.240	29	WP76
WP39	30	57.695	57 41.700	326.953	33 02.820	57.550	57 33.000	327.455	32 32.700	30	WP40
WP5	31	57.683	57 40.980	326.941	33 03.540	57.531	57 31.860	327.473	32 31.620	31	WP4
WP78	32	57.672	57 40.320	326.923	33 04.620	57.519	57 31.140	327.461	32 32.340	32	WP77
WP38	33	57.659	57 39.540	326.917	33 04.980	57.507	57 30.420	327.449	32 33.060	33	WP37
WP2	34	57.664	57 39.840	326.845	33 09.300	57.494	57 29.640	327.437	32 33.780	34	WP3
WP26	35	58.054	58 03.230	327.251	32 44.940	57.597	57 35.820	327.083	32 55.020	35	WP27
WP29	36	58.031	58 01.838	327.332	32 40.080	57.575	57 34.500	327.161	32 50.340	36	WP28
WP30	37	58.010	58 00.568	327.408	32 35.520	57.552	57 33.120	327.240	32 45.600	37	WP31
WP33	38	57.987	57 59.243	327.485	32 30.900	57.530	57 31.800	327.317	32 40.980	38	WP32
WP34	39	58.000 via	58 00.000	327.609	32 23.460	57.508	57 30.480	327.395	32 36.300	39	WP36
WP35		57.701	57 42.060	327.466	32 32.040						
		new									
	32	57.666	57 39.930	326.920	33 04.800	57.513	57 30.780	327.455	32 32.700	32	
	8	57.959	57 57.540	327.182	32 49.080	57.815	57 48.900	327.684	32 18.960	8	
		deleted									
	9										
	33										
		modified									
	20	57.813	57 48.800	327.077	32 55.400	57.573	57 34.380	327.904	32 05.760	20	

Shooting order / line	Heading/shooting direction	Comments
34	SE	
31	NW	
28	SE	Sonobuoy A
25	NW	
22	SE	
19	NW	
16	SE	Sonobuoy B
13	NW	
10	SE	
7	NW	
4	SE	
1	NW	
2		*
5		
36/1	N	Sonobuoy C, D, E
37	S	Sonobuoy F, G
38	N	Sonobuoy H, I
39/1	S	Sonobuoy J, K, L
15	NW	
20	SE	Q - 57 49.240 / 32 57.328 R - 57 40.649 / 32 27.227
17	NW	
14	SE	
18	NW	
21	SE	
24	NW	
27	SE	
30	NW	
32 New	SE	
29	NW	
26	SE	
23	NW	
12	SE	
8 New	NW	turn to stbd along line 36
36/2	S	S - 57 58.054 / 32 41.445
39/2	N	turn to stbd along line 6
6/1	SE	
3	NW	
6/2	SE	T - 57 52.811 / 32 24.000
11	NW	U - 57 48.000 / 32 24.000
35		

Leaving lines below unshot

9
33

* Note this turn requires *light bulbing* or *fish tailing* as is tighter than 4°/min.

Table 5
XBT deployment positions

Station number	Probe type	Probe s/n	Latitude (N)	Longitude (W)	Day	Time (GMT)	Depth	Comments
001	T5	260928	57 30.23	32 36.20	202	20:15	1704	Failed
002	T5	260929	57 29.90	32 34.80	202	20:26	1798	Failed
003	T5	260932	57 43.20	32 51.80	203	09:50	1448	Failed after 350m
004	T5	260933	57 52.30	32 19.90	205	13:31	1810	Failed at launch
005	T5	260934	57 53.10	32 22.60	205	13:50	2000	Failed to receive
006	T5	260935	57 57.00	32 36.30	205	15:38	1693	OK to 1700m
007	T5	260936	57 37.00	33 21.20	211	00:06	1497	OK to 1280m
008	T5	260938	57 35.90	33 10.80	211	00:36	1630	Record failed - computer drive failure
009	T5	260939	57 34.90	33 01.60	211	01.00	1895	OK to 1180m
010	T5	260988	57 34.40	32 57.50	211	01.11	2074	Failed
011	T5	260992	57 34.00	32 54.50	211	01:20	2207	OK to 1240m
012	T5	260996	57 33.70	32 51.60	211	01:27	2168	OK to 1170m
013	T5	260989	57 33.40	32 48.50	211	01:36	2034	OK to 1110m
014	T5	260990	57 33.10	32 45.40	211	01:44	1993	OK to 1190m
015	T5	260991	57 32.80	32 42.50	211	01:52	2018	OK to 1170m
016	T5	260993	57 32.50	32 39.10	211	02:02	1647	OK to 1160m
017	T5	260994	57 32.10	32 34.20	211	02:14	1534	OK to 1160m
018	T5	260995	57 31.70	32 30.00	211	02:26	1756	OK to 1190m
019	T5	260997	57 31.20	32 24.70	211	02:40	1527	OK to 1200m
020	T5	261076	57 30.60	32 19.70	211	02:55	1443	OK to 1220m
021	T5	261077	57 30.20	32 15.90	211	03:06	1740	OK to 1220m
022	T5	261078	57 29.50	32 11.10	211	03:20	1566	OK to 1270m
023	T5	261079	57 29.10	32 00.60	211	03:27	1723	OK to 1230m
024	T5	261080	57 28.50	32 03.20	211	03:42	1981	OK to 1200m
025	T5	261081	57 28.10	31 59.30	211	03:54	1816	OK to 1290m
026	T5	261082	57 27.80	31 56.30	211	04:02	1783	OK to 1260m
027	T5	261083	57 27.40	31 52.20	211	04:14	1751	OK
028	T5	260998	57 08.10	30 38.20	211	10:00	1750	Failed
029	T5	260999	57 08.10	30 38:20	211	11:43	2309	Failed

Table 6
Cruise statistics

Downtime

(hard to quantify exactly - as considered gradational down from specified parameters)

Total line length planned (not inc. turns)	=	1685 km	
Total line length after shortening due to definition of arrival day	=	1447 km	
Total line length actually shot	=	1333 km	= 79%

Grade A downtime (worst kind)

No. line kms not shot at all	=	114	= 7%
Length of line lost due to shortening of programme	=	238	= 14%

Grade B downtime

Total length of line **NOT** shot with specified airgun source and/or multichannel streamer at specified depths	=	1333 km	= 100%

Grade C downtime

Length of line shot without full compressor capability	=	1220	= 84%
Length of line shot with the following no. of guns down		1) 456	= 32%
		2) 278	= 19%
		3) 204	= 14%
		4) 26	= 2%
		5) 0	= 0%
		6) 0	= 0%
		7) 0	= 0%
		8) 22	= 2%
		9) 0	= 0%
		10) 0	= 0%
		11) 0	= 0%
		12) 18	= 1%
		TOTAL	= 70%

shot with sub-specification source power